# Are glacial refugia hotspots of speciation and cyto-nuclear discordances? Answers from the genomic phylogeography of Spanish common frogs

Christophe Dufresnes[1,2], Alfredo G. Nicieza[3,4], Spartak N. Litvinchuk[5,6], Nicolas Rodrigues[7], Daniel L. Jeffries[7], Miguel Vences[8], Nicolas Perrin[7], and Íñigo Martínez-Solano[9]

[1] College of Biology and Environment, Nanjing Forestry University, Nanjing, China.

[2] Department of Animal and Plant Sciences, University of Sheffield, Sheffield, United Kingdom.

[3] Department of Organisms and Systems Biology, University of Oviedo, Spain.

[4] Research Unit of Biodiversity (UMIB, CSIC-UO-PA), University of Oviedo, Spain.

[5] Institute of Cytology, Russian Academy of Sciences, Saint Petersburg, Russia.

[6] Dagestan State University, Makhachkala, Russia.

[7] Department of Ecology & Evolution, University of Lausanne, Lausanne, Switzerland.

[8] Zoological Institute, Technische Universität Braunschweig, Braunschweig, Germany.

[9] Departamento de Biodiversidad y Biología Evolutiva, Museo Nacional de Ciencias Naturales (MNCN-CSIC), Madrid, Spain.

**Running head**: Genomic phylogeography of common frogs

**Abstract**

Subdivided Pleistocene glacial refugia, best known as “refugia within refugia”, provided opportunities for diverging populations to evolve into incipient species and/or to hybridize and merge following range shifts tracking the climatic fluctuations, potentially promoting extensive cyto-nuclear discordances and “ghost” mtDNA lineages. Here we tested which of these opposing evolutionary outcomes prevails in northern Iberian areas hosting multiple historical refugia of common frogs (*Rana* cf. *temporaria*), based on a genomic phylogeography approach (mtDNA barcoding and RAD-sequencing). We found evidence for both incipient speciation events and massive cyto-nuclear discordances. On the one hand, populations from northwestern Spain (Galicia and Asturias, assigned to the regional endemic *R. parvipalmata*), are deeply-diverged at mitochondrial and nuclear genomes (~4My of independent evolution), and barely admix with northeastern populations (assigned to *R. temporaria* sensu stricto) across a narrow hybrid zone (~25km) located in the Cantabrian Mountains, suggesting that they represent distinct species. On the other hand, the most divergent mtDNA clade, widespread in Cantabria and the Basque country, shares its nuclear genome with other *R. temporaria* s. s. lineages. Patterns of population expansions and isolation-by-distance among these populations are consistent with past mitochondrial capture and/or drift in generating and maintaining this ghost mitochondrial lineage. This remarkable case study emphasizes the complex evolutionary history that shaped the present genetic diversity of refugial populations, and stresses the need to revisit their phylogeography by genomic approaches, in order to make informed taxonomic inferences.

**Keywords**: ghost lineage, glacial refugium, hybrid zone, *Rana parvipalmata*, *Rana temporaria*, RAD-sequencing.

## Introduction

Cases of cryptic divergence between evolutionary lineages are increasingly discovered across groups of organisms, with important implications for biodiversity and taxonomic assessments (Avise 2000, Jörger & Schrödl 2013, Struck et al. 2018, Chenuil et al. 2019). Indeed, half of all the scientific publications registered in the Web of Knowledge database with the key word "cryptic species" have been published just within the last six years (Web of Knowledge 2019). Species or lineages are typically defined as cryptic if they show substantial evolutionary – typically genetic – divergence yet cannot be readily distinguished by morphology. Several areas with a rich tectonic and climatic history have been highlighted as potential hotspots for cryptic speciation. For instance, in southern European peninsulas, complex topographic features favored events of deep allopatric divergences, as well as lineage persistence during the ensuing Pleistocene climatic fluctuations in "refugia within refugia" (Hewitt 1996, Gómez & Lunt 2007, Provan & Bennett 2008). Accordingly, many closely-related endemics have been tentatively described from Mediterranean refugia (e. g. Díaz-Rodríguez et al. 2017, Dufresnes et al. 2018, 2019a).

Despite a large number of publications referring to these refugia, the detailed biogeographic processes by which they contribute to forming new lineages and species are incompletely understood. Recuero & García-París (2011) formalized a fundamental difference of types of refugia: (i) previously unoccupied areas into which lineages retreat once their original range becomes unsuitable due to climate change (true refugia), and (ii) areas that remained climatically suitable, and where lineages persisted throughout episodes of climatic change such as glacial cycles (sanctuary-type refugia). Furthermore, glacial cycles would differentially affect species depending on their ecological preferences, i. e. cold-adapted species would retreat into northern and montane areas during warm interglacials, and undergo range expansions southwards and into lowlands during glacials (Sánchez-Montes et al. 2019), while warm-adapted species will thrive during interglacials and retreat southwards and into lowlands during glacials (Stuart et al. 2009, Gutiérrez-Rodríguez et al. 2017a, 2017b). Consequently, beyond the classic major refugial areas (Hewitt 1996; Schmitt 2007; Stuart et al. 2009), microrefugia have promoted species persistence in regions experiencing high climatic turnover through time, shaping local patterns of genetic diversity (Schmitt & Varga 2012).

In parallel, ascertaining the complex history of refugia and whether they led to cryptic speciation events remains challenging with the nuclear loci that have been traditionally used in phylogeography and population genetics. For instance, microsatellites may lack diagnostic variation between phylogeographic lineages because of allele homoplasy and ancestral polymorphism, while small sets of intronic sequences

feature too few variable sites. Consequently, the delimitation of cryptic taxa has extensively relied on mitochondrial DNA (mtDNA) divergences (Krishnamurthy & Francis 2012). However, it is now well-established that deep mtDNA lineages do not always represent significant population divergences (Zink & Barrowclough 2008, Collins & Cruickshank 2012, Morgan-Richards et al. 2017), and even when they do, whether they kept diverging independently or faded away by recurrent episodes of admixture often remains an open question (Garrick et al. 2019).

Another major issue with over-reliance on mtDNA is the prevalence of cyto-nuclear discordances across taxa (Toews & Brelsford 2012, Bonnet et al. 2017), which can lead to false evolutionary and taxonomic conclusions ("mirage of cryptic species", Hinojosa et al. 2019). Cyto-nuclear discordances may have selective causes (local adaptation of mtDNA genes, Pavlova et al. 2013; asymmetric hybridization, Chan & Levin 2005), but they often result from neutral demographic processes, e.g. faster rate of molecular evolution and lower effective sizes of mitochondrial DNA (Rosenberg 2003), sex-biased dispersal (e.g. Dai et al. 2013), or mitochondrial introgression or fusion following secondary contacts (e. g. Phuong et al. 2017, Garrick et al. 2019). Theoretical (Currat et al. 2008, Excoffier et al. 2009) and empirical data (Cahill et al. 2013, Phuong et al. 2017) have shown that demographic expansions at range margins can promote asymmetric gene flow in the initial stages of the contact (from the local to the expanding taxa), traces which are expected to persist longer in the mitochondrial than in the nuclear genome. Consequently, it has been proposed that cyto-nuclear discordances may preferentially occur in regions subjected to climate instability (Phuong et al. 2017), where frequent range shifts offered recurrent opportunities for lineages to expand and admix.

Under these assumptions, we posit that subdivided glacial refugia, where regionally diverged lineages recurrently expanded and hybridized during the succession of glacial-interglacial periods, could also be candidate hotspots for extensive cyto-nuclear discordances. For instance, a large part of the genetic diversity of terrestrial vertebrates originates from admixture and/or fusion between young refugial lineages (Petit et al. 2003, Canestrelli et al. 2014), forming "evolutionary melting pots" (Dufresnes et al. 2016). This implies that the lineages found across separate glacial refugia could have experienced frequent events of hybridization, and, in turn, that the mitochondrial phylogeographies from these regions might be unreliable. It is therefore essential that taxonomists and conservation biologists comprehensively sample both mitochondrial and nuclear genomes to account for the possibility of cryptic species, which would otherwise not be revealed (Struck et al. 2018, Chenuil et al. 2019).

Phylogeographic surveys using high-throughput sequencing techniques can provide unprecedented insights into the history of lineages affected by Pleistocene climatic fluctuations. By clarifying the evolutionary relationships of young species complexes, and thoroughly assessing admixture between closely-related lineages, the nascent field of "genomic phylogeography" can inform on suspicions of cryptic speciation (e. g. Dufresnes et al. 2019a, 2020, Hinojosa et al. 2019), and even characterize super-cryptic species, i. e. cryptic species where mtDNA barcoding is unreliable (Dufresnes et al. 2019b). Fine-scale genomic phylogeographies can accurately map cyto-nuclear discordances, and help assess whether refugial populations experienced mitochondrial capture, lineage fusion, ephemeral mitochondrial divergences, or represent evolutionary significant units on the verge of speciation.

Here we ask whether refugial areas in northern Iberia are hotspots of cryptic speciation or of cyto-nuclear discordances in the European common frog (*Rana temporaria*). This very adaptable species is widespread throughout Europe, and retained a large southern distribution during the last glacial stage (Vences et al. 2013), including northern Iberia, where it has a rich Quaternary fossil record (Lobo et al. 2016). At least five deeply-diverged mtDNA clades coexist across Galicia (T1), Asturias (T1, T2), Cantabria (T2, T6), the Basque country (T6, T4) and the Pyrenees (T4, T3) (Vences et al. 2013, 2017). Such strong mitochondrial structure is consistent with the existence of several refugia within the Iberian refugium, but the nuclear diversity of populations remains poorly understood. Using allozymes, Arano et al. (1993) and Veith et al. (2002, 2012) mapped two widely-admixing genetic clusters tentatively assigned to subspecies *R. t. temporaria* (east) and *R. t. parvipalmata* (west), which however did not match the distribution of the main mtDNA lineages. Based on protein-coding sequences of the nuclear gene RAG-1, Vences et al. (2013) identified private haplotypes for only the westernmost lineage (T1). Interestingly, unlike many other ectothermic taxa for which southern refugia/sanctuaries have been hypothesized, *R. temporaria* tolerates cold conditions – it has the northernmost range boundary known among European amphibians (even reaching the subarctic belt) and the highest altitudinal records (e. g. Vences et al. 2002). Hence, its refugial diversity could have been shaped by expansions during the long glacial periods, but constrictions during interglacials, opposing the classical patterns known from most ectotherms. Disentangling these processes and resolving the phylogeography and systematics of *R. temporaria* in the Iberian refugium is thus pending more comprehensive analyses of nuclear genomic data sets, especially in the light of potential cyto-nuclear discordances.

In this study, we applied a RAD-sequencing approach for anuran population genomics (Brelsford et al. 2016) to reconstruct the phylogeographic history of *R. temporaria* across its refugial ranges in northern Spain. Combining species distribution modeling (SDM) with mtDNA and genome-wide nuclear

data from hundreds of individuals, we first aimed to understand whether the deeply-diverged mitochondrial lineages correspond to reciprocal nuclear lineages that persisted throughout the glacial cycles. Second, we tested whether the identified transitions could be consistent with reproductive isolation and thus incipient speciation. Third, we investigated the proximate causes of the cyto-nuclear discordances documented, by testing whether and how the distribution of genetic diversity and of discordant lineages may be associated to their predicted ecological preferences and their demographic expansions during the Quaternary climatic fluctuations.

## Methods

### *Sampling, laboratory and bioinformatic procedures*

Tissue samples were collected from 340 individuals captured across northern Spain (41 localities), using buccal swabs, toe clips (adults) or tail tips (tadpoles), stored in 70–96% of ethanol and/or frozen at -20°C. Animal captures were sanctioned by collecting permits as follows: Diputación Foral de Gipuzkoa (exp.: 2364); Diputación Foral de Bizkaia (exp.: 8-2017); Diputación Foral de Álava (exps.: 17/014, 17/18); Gobierno de Navarra (exp.: 240/17); Principado de Asturias (2006/000223, 2008/000272, 2010/000371, 2016/001092, 2017/001208, 2017/019842, 2018/001076, 2018/007781), Parque Nacional Picos de Europa (CO/09/0032/2005, CO/09/0007/2006, CO/09/646/2006, CO/09/077/2009, CO/09/0571/2009, CO/09/041/2011, CO/09/121/2012, CO/09/0125/2013, CO/09/012/2014, CO/09/065/2015, CO/09/0316/2015, PNP-1096/17-SCN, CO/09/073/2018, PNP-471/2018-SCN), Junta de Castilla y León (EP/CYL/389/2007, EP/LE/428/2010, EP/P/428/2010, EP/CYL/31/2010, EP/P/426/2010, EP/CYL/625/2013, EP/CYL/725/2015, EP/CYL/112/2017), Gobierno de Cantabria (EST-275/2016-SEP, EST-81/2017-SEP, EST-75/2018-SEP), Xunta de Galicia (560/2011), and Conselh Generau d'Arán (75/CS/10/2010). DNA was extracted using the BioSprint robotic workstation (Qiagen). Details on the samples analyzed in this study can be found in File S1a.

To map the mitochondrial lineages, all samples were DNA-barcoded using the primer pair CytB-F2 / CytB-R2 (Dubey et al. 2019), which specifically amplifies ~550bp of the highly variable gene *cytochrome-b* in ranids (see methods therein). Sequences were aligned in SeaView 5 (Gouy et al. 2010) and assigned to the main mitochondrial lineages documented by Vences et al. (2017). For the majority of individuals ($n$ = 331 from the 41 populations), 501bp could be analyzed and assigned to haplotypes. Additionally, we also included haplogroup frequencies for an additional 137 populations from Vences et al. (2013, 2017). Haplogroup frequencies at these 178 populations are available in File S1b.

For the genome-wide nuclear data, we prepared a double digest RAD (ddRAD) multiplexed library for 261 samples (from 33 localities, see File S1), following the methodology of Brelsford et al. (2016). The library was sequenced on three Illumina HiSeq 2500 lanes (single read 125) and raw sequences were demultiplexed with Stacks v1.48 (Catchen et al. 2013). We used the *denovo.pl* pipeline with default parameters (*–M* 2, *–m* 3 and *–n* 2) to catalog the tags sequenced in each sample, including additional RAD sequence reads from five individuals of *R. arvalis* (a close relative of *R. temporaria*) obtained with the same protocol (Brelsford et al. 2017), to be used as outgroups (Rarv49, Rarv70, Rarv92, Rarv66, Rarv81). For population genomic analyses across northern Spain, SNPs (Single Nucleotide Polymorphism) were called from RAD tags (118bp sequences) sequenced in all populations (*–p* 33) and in all samples of each (*–r* 1), while discarding those bearing rare variants (*–min_maf* 0.05) and those that were predominantly heterozygous (*–max_het_obs* 0.75), which can represent overmerged paralogs. To further investigate substructure and demographic trends within the main nuclear clusters identified (see Results), we also called SNPs among individuals from localities 4–16 (western group T1–T2, $n = 97$), from localities 11–16 (T2 only, $n = 49$), and localities 26–41 (eastern group T6+T4, $n = 92$), without missing data. For phylogenetic analyses, we outputted RAD tags and SNPs genotyped among 30 *R. temporaria* individuals representative of the northwestern Spanish nuclear and mitochondrial diversity, and far away from the areas of admixture (see File S1a and Results), together with the five *R. arvalis* samples.

*Population genetics*

The nuclear genetic structure of common frogs across northern Spain was first assessed from 566 SNPs (representing 469 RAD tags) present in all 261 individuals analyzed. We performed a Principal Component Analysis (PCA) using *adegenet* (Jombart 2008) and assigned individual genotypes to clusters with STRUCTURE (Pritchard et al. 2000). For the latter, chains were run for $K = 1–8$, each of 100,000 iterations after a burnin of 10,000, without prior information on sample origin. We also computed observed heterozygosity and a tree of pairwise genetic distances ($F_{st}$) between populations, using *hierfstat*. In parallel, the nucleotide diversity ($\pi$) of *cyt-b* was computed for each population with $n \geq 5$.

Furthermore, we fitted sigmoid clines to the nuclear ancestry (STRUCTURE Q) and the mitochondrial frequency data across the geographic transition between the two main genetic groups identified in our study area (T1+T2 and T6+T4), with *hzar* (Derryberry et al. 2014). The transect extended longitudinally along localities 11–28 (see Results), and geographic distances were measured in Google

Earth (https://earth.google.com). We tested models from two (cline center *c* and cline width *w*) to up to eight parameters, and selected those with the highest AIC scores.

Patterns of genetic differentiation within groups were assessed by PCAs, namely localities 4–16 (T1–T2; 5,354 SNPs representing 4,083 RAD tags), localities 11–16 (T2 only; 9,930 SNPs on 7,157 RAD tags) and localities 26–41 (T6+T4; 997 SNPs representing 806 RAD tags). Note that the nuclear group T1 was not analyzed separately because a single population was sequenced. To test for isolation-by-distance, we computed pairwise genetic ($F_{st}$; *hierfstat*) and geographic distances between populations (Geographic Distance Matrix Generator 1.2.3, available at: http://biodiversityinformatics.amnh.org/open_source/gdmg/index.php). The obtained matrices were then compared using Mantel tests (function *mantel.rtest* from *ade4*, with 10,000 bootstraps).

*Phylogenetic analyses*

For the mitochondrial phylogeny, we harvested sequences of six genes and stretches of tRNA (totaling 4,278bp) from Vences et al. (2017) for 18 individuals of *R. temporaria* representative of all the mtDNA clades reported across the ranges (T1–T6, including subclades of T4), as well as one individual of *R. arvalis*. Details are available in File S1c. For the nuclear phylogeny, our alignment (30 Spanish *R. temporaria* and five *R. arvalis*) comprised 1,207 concatenated RAD tags (~142kb). Phylogenetic analyses were performed by maximum-likelihood with PhyML 3.0 (Guidon et al. 2010), using the smart model selection method (SMS) with AIC criterion (Lefort et al. 2017), and 100 bootstrap replicates to assess node significance.

Second, to estimate divergence times, we analyzed subsets of these two alignments in BEAST, retaining 1-2 samples per clade/subclade (list in File S1a, S1c). We used birth-death models for the tree priors and applied relaxed lognormal clocks calibrated at 12.5 ± 1.0 Mya for the tree roots (normal distributions), i. e. the estimated split between *R. temporaria* and *R. arvalis* (Yuan et al. 2016). For mtDNA, site models were adapted from Vences et al. (2017), and we applied a GTR + G model to the nuclear data (inferred with bModeltest, Bouckaert & Drummond 2017). Chains were run for 50 million iterations, sampling trees every 5,000, and visualized using the software DensiTree (Bouckaert & Drummond 2014), discarding the first 20% as burnin. Stationarity and convergence were checked using Tracer 1.5 (available at: http://beast.community/).

We further reconstructed species trees from our nuclear SNP alignment (3,157 SNPs) under the Bayesian framework of SNAPP (Leaché et al. 2014) implemented in BEAST 2 (Bouckaert et al. 2014). Model parameters and priors were optimized following the recommendations of Leaché & Bouckaert (2018). The chain was sampled every 1,000 iterations, ran for about 4 million iterations, and stopped after long-term stationarity and large effective sample sizes of parameters (>200). Results were visualized by cloudogram in Densitree 2.0 (Bouckaert and Heled, 2014), with a burnin of 20%.

Finally, to get a finer view of mitochondrial relationships across northern Spain, we also produced a haplotype network of the hypervariable *cyt-b* sequences (501bp) of our samples ($n$ = 331), using the R package *pegas* (Paradis 2010).

*Demographic analyses*

Bayesian demographic reconstructions of effective population sizes through time were performed with the Extended Bayesian Skyline Plot (EBSP) model implemented in BEAST (Heled & Drummond 2008), separately for the two main genetic groups identified (see Results). Note that because of the large amount of data, we restricted the analyses to variable sites only, instead of full sequences, which otherwise represent millions of base pairs. For the eastern group, we considered the nuclear (997 SNPs, $n$ = 92) and mitochondrial data (501bp of *cyt-b*, $n$ = 122) sequenced for localities 26–41, which correspond to the nuclear T6+T4 cluster. For the western group, we considered the nuclear (9,930 SNPs, $n$ = 49) and mitochondrial data (501bp of *cyt-b*, $n$ = 60) sequenced for localities 11–16, which correspond to pure populations of lineage T2. Because demographic reconstructions are sensitive to population structure (Heller et al. 2013), we did not include the genetically differentiated T1 samples, nor admixed individuals in the analysis.

For both analyses, we applied models of sequence evolution as above, and the nuclear substitution rates were estimated from the mitochondrial rate, which was fixed to the values obtained for *cyt-b* in the time-calibrated phylogeny (0.01168 substitutions / bp / My). Priors and operators were optimized following EBSP recommendations for BEAST 2 (available at https://www.beast2.org/tutorials/). Chains were run for 100 million iterations, sampling every 10,000, and checked with Tracer. The final skyline plots were obtained using a custom R script (available at: https://www.beast2.org/tutorials/), discarding the first 20% of trees as burnin.

*Species distribution modelling*

To get insights on the possible extent of the range of *R. temporaria* across northern Spain throughout the Late-Quaternary, we built species distribution models (SDMs) projected under past environmental conditions with Maxent 3.4.1 (Phillips et al. 2006). We performed three sets of analyses, based on (1) all genetic groups combined (*R. temporaria* sensu lato); (2) separately for the two main genetic groups (western clade T1–T2, and eastern clade T3–T6); and (3) specifically for the mtDNA lineages T6 and T4 in northwestern Spain, as a way to test whether adaptation to different ecological niches could explain their persistence, despite the absence of reciprocal nuclear divergence (see Results).

For the contemporary niche predictions, we gathered 5,109 localities of *R. temporaria* from our own and published records (File S1d, mapped on File S2). Filtering was performed with ENMTools 1.3 (Warren et al., 2010) to avoid spatial autocorrelation and duplication of occurrence points. For present-time predictions, altitude and 19 bioclimatic layers summarizing the past fifty years (~1950–2000) were extracted from the WorldClim 1.4 database (http://www.worldclim.org). An additional seven layers were considered: three from online databases (aridity index, http://www.cgiar-csi.org/data/global-aridity-and-pet-database; spatial homogeneity of global habitat, http://www.earthenv.org/texture.html; global percent of tree coverage, https://github.com/globalmaps/gm_ve_v1) and four topographic layers (aspect, exposition, slope, and terrain roughness index) calculated with QGIS (http://www.qgis.org/). All of them featured 30 arc-seconds spatial resolutions. The mask applied extends from 35 N° to 73° N and 13° W to 75° E.

For predictions at the Last Glacial Maximum (LGM; ~21,000 years ago) and the Last Interglacial (LIG; ~120,000-140,000 years ago), bioclimatic layers were extracted from the WorldClim and PaleoClim (paleoclim.org/) databases, respectively (2.5 arc-minutes spatial resolution). Two general atmospheric circulation models were used to generate LGM climate scenarios: the Community Climate System Model (CCSM; http://www2.cesm.ucar.edu/) and the Model for Interdisciplinary Research on Climate (MIROC; Watanabe et al. 2011).

To eliminate predictor collinearity prior to generating the model, we calculated Pearsons's correlation coefficients for all pairs of bioclimatic variables using ENMTools. We excluded the variable of a correlated pair with $|r| > 0.75$ that we considered to be the less biologically important, based on known preferences of *R. temporaria*. The resulting dataset contained seven bioclimatic variables: Bio1 (annual mean temperature; °C×10), Bio2 (mean diurnal range; °C×10), Bio7 (temperature annual range; °C×10), Bio8 (mean temperature of wettest quarter; °C×10), Bio12 (annual precipitation; mm), Bio15

(precipitation seasonality; CV), and Bio18 (precipitation of warmest quarter, mm). A total of 15 variables were thus used in the models.

Model performance was assessed by the Area Under the Curve (AUC) derived from the Receiver Operating Characteristic (ROC) plots. AUC values range from 0.5 to 1.0, with 0.5 indicating no greater fit than expected by chance and 1.0 indicating a perfect model fit. AUC values above 0.75 are considered useful and above 0.90 very good (Swets 1988; Elith et al. 2000). We used default settings in MaxEnt (30 replicates), i.e. regularization multiplier of 1.0, all feature classes, maximum iterations 500 and maximum number of background points 10,000 (Phillips and Dudík, 2008). We applied a jackknife analysis for estimating the relative contributions of variables to the MaxEnt model. Finally, the niche overlap between target lineages was estimated by Schoener's D distance in ENMTools, and by a PCA on the 15 retained geoclimatic variables at occurrence localities (R package *ade4*).

To understand whether changes in past and present distributions affected genetic diversity, admixture and cyto-nuclear discordances, we performed a series of statistical comparisons among different pairs of interacting lineages. First, we outputted the probabilities of occurrence under each of the four climatic scenarios at 33 populations where we genotyped ≥5 frogs, and calculated the standard deviation between present, LGM and LIG probabilities as a proxy to climatic instability. For the LGM, the MIROC and CCSM models yielded similar and highly correlated results, and we considered the MIROC estimates in the comparisons. As a proxy to admixture, we transformed the average assignment to one nuclear cluster $x$ ($Q_x$, taken from the STRUCTURE's $Q$) into an admixture index AI ranging from 0 (no admixture) to 0.5 (intermediate assignment), as $\min(Q_x, 1\text{-}Q_x)$. As a proxy to cyto-nuclear discordances, we computed the deviation $D$ between $Q_x$ and the frequency ($P_x$) of the corresponding mtDNA lineage (T1-T2 or T4+T6), as $D = \left| Q_x\text{-}P_x \right|$. Relationships were tested by linear regressions in *R*, with thresholds of significance adjusted with Bonferroni corrections for multiple tests.

## Results

*Genetic structure and diversity*

Based on *cyt-b* sequences, we recovered and mapped four main mitochondrial lineages throughout northern Spain, from west to east: T1 (pink), T2 (orange), T6 (light blue) and T4 (blue) (Fig. 1A; see haplotype network in File S3a). T1 was further divided into two monophyletic sublineages endemic to Galicia (T1a, pink) and western Asturias (T1b, light pink), respectively (File S3a, Fig. 1A). Our dense

sampling combined with the data of Vences et al. (2013, 2017) allowed to accurately locate the mitochondrial transitions, which involved syntopy of lineages at several localities in western Asturias (T1/T2) and the Basque country (T6/T4), and at a single site in western Cantabria (T2/T6) (Fig. 1A).

The nuclear variation (566 SNPs) was summarized into two main genetic clusters (Fig. 1B, Fig. 2). The first one (orange) is restricted to the western parts of the Atlantic coast in the regions of Galicia and Asturias, and corresponds to mtDNA lineages T1+T2 (Fig. 1). The second one (blue) inhabits the eastern parts of the Cantabrian ranges (Cantabria and Basque country) and corresponds to mtDNA lineages T6+T4 (Fig. 1). Their strong nuclear differentiation is highlighted by PC1 on the PCA (>40% of the total genetic variation, Fig. 2), $K = 2$ as the best STRUCTURE solution ($\Delta K = 8018.6$; File S4), and the strongest pairwise $F_{st}$ between populations (File S5). The two groups form a narrow hybrid zone at the border between Cantabria and Asturias (loc. 17–24), where the majority of admixed individuals carries T6 mtDNA (loc. 21–23) (Figs. 1–2). This cyto-nuclear asymmetry is reflected by cline analyses along our transect spanning localities 11–28 (Fig. 3), where the mitochondrial cline center ($c = 68.0$km) is shifted about ten kilometers west compared to the nuclear cline center ($c = 77.7$km), with non-overlapping confidence intervals (CI), i. e. mtDNA: 66.5–70.8km, nuclear: 73.1–84.4km. Both clines were sharp, with width $w = 14.9$km for mtDNA (CI: 11.5–24.3km; only a single population with syntopic mtDNA lineages sampled) and $w = 25.0$km for nuclear loci (CI: 18.2–38.9km). Across northern Spain, most of the genetic diversity was found at lineage transitions for mtDNA (based on *cyt-b*; Fig. 4A) and nuclear markers (based on 566 SNPs; Fig. 4B).

Within the western cluster, our main nuclear dataset (566 SNPs) differentiated between Galician (corresponding to mtDNA lineage T1) and Asturian populations (corresponding to mtDNA lineage T2), as seen from PC2 of the PCA (Fig. 2) and the STRUCTURE analyses with $K = 3$ (Fig. 1B). The complementary dataset restricted to T1–T2 (5,324 SNPs) yielded a similar picture, with the two subgroups admixing in western Asturias (loc. 6–10) (File S6a). Within the well-sampled Asturian subgroup (T2, loc. 11–16; 9,930 SNPs), individuals clustered by localities (File S6a), with no obvious link between genetic and geographic distances (Mantel test, $r = 0.19$, $P = 0.30$).

Within the eastern cluster, and despite strong mitochondrial differentiation (T6 *vs* T4), no structure stands out from our main nuclear dataset (Fig. 2): increasing $K$ up to $K = 8$ did not improve the run likelihoods (File S4), and these populations always remain as a single cluster. Complementary analyses restricted to localities 26–41 (997 SNPs) also grouped individuals by populations, or sets of nearby populations (File S6b), with significant isolation-by-distance (Mantel test, $r = 0.53$, $P < 0.001$).

Combining nuclear with mitochondrial data, we recovered clear signals of population expansions among the western (T2) and the eastern groups (T6+T4) during the Late-Pleistocene (Fig. 4C). In both cases, the analyses depicted a >100 fold increase of effective population size, initiated at the beginning of the last glaciation (~100kya).

*Phylogenetic analyses*

Built from six genes (4,278bp) taken from Vences et al. (2017), the maximum-likelihood mitochondrial phylogeny suggested successive splits of the branches leading to T6, T1/T2, T3 (restricted to the Spanish Pyrenees), T4 and T5 (restricted to far-eastern ranges), respectively (File S3b; sketched on Fig. 1A for the northern Spanish lineages). The time-calibrated analyses in BEAST confirmed the topology (File S3c) and suggested a Plio-Pleistocene diversification initiated around 2.5Mya (95% HPD = 1.9–3.2My).

Based on maximum-likelihood (~142kb of concatenated RAD tags) and SNAPP (3,157 SNPs), the nuclear phylogenies (File S3d; sketched on Fig. 1B) confirmed a deep split between the two main clades present in northwestern Spain (T1 and T2 *vs* T6 and T4). According to our time-calibrated tree (File S3c), their divergence was estimated to the Pliocene (4.1My, 95% HPD = 2.3–6.2My). Samples belonging to mitochondrial lineages T6 and T4 form a single nuclear clade, while those belonging to mtDNA lineages T1 and T2 formed distinct monophyletic nuclear subclades, respectively (File S3d). The latter split was estimated at 2.1Mya (95% HPD = 1.1–3.3My).

*Species distribution modelling*

The SDMs performed better for the western (T1–T2, AUC > 0.99) compared to the eastern clade (T3–T6, AUC = 0.80), most likely due to the widespread and ecologically heterogeneous ranges occupied by the latter (File S7). The latter model was very similar to the one from both groups combined, since it was built from mostly the same localities. Putative distributions under present, glacial (CCSM) and last-interglacial conditions are displayed in Fig. 5; all projections are available as supplementary material (File S8a). Overall, the suitability of Cantabrian ranges improved during the last glacial stage for both groups (Fig. 5, File S8a). The area of contact seemingly offered suitable conditions for common frogs prior and after the LGM (Fig. 5, File S8a). For each clade separately, or both of them combined, the probabilities of occurrence under any climate scenario, and the variance between the three modeled periods, were not significant predictors of the nuclear ($H_o$) and mitochondrial ($\pi$) diversity, neither of the amount of

admixture (AI) between parapatric populations, or of the cyto-nuclear discordances (*D*), after Bonferroni corrections (File S9).

According to Schoener's D, niche overlap was low between the two main clades (D = 0.15), although the two niches are not disruptive according to the predicted ranges (Fig. 5, File S8a) and the first components of the PCA (File S10). Occurrence records are climatically very heterogeneous for the widespread eastern clade (File S10), and the most important variables in the climatic model were the aridity index (67.7%), the annual temperature range (Bio7; 11.8%) and the mean diurnal temperature range (Bio2; 7.7%). The annual temperature range (Bio7) was also among the main contributors in the model of the western clade (41.3%), followed by slope (20.3%) and precipitation of the warmest quarter (Bio18; 13.6%).

The SDMs built separately for mtDNA lineages T6 and T4 received high AUC scores (File S7) and did not predict disruptive potential distributions: the Spanish Atlantic coast and the Pyrenees have remained suitable for both lineages under LGM and present conditions (File S8b). Accordingly, niche overlap was high (Schoener's D = 0.48), and both lineages encompass the same climatic space on the PCA (File S10). Moreover, the same variables significantly contributed to both models: temperature annual range (Bio7, T4: 40.3% and T6: 35.9%), slope (T4: 15.3%, T6: 35.4%), and the aridity index (T4: 17.7%, T6: 13.1%).

## Discussion

### *Cryptic speciation in a sanctuary-type refugium*

Following up on Vences et al. (2013), our genetic and bioclimatic analyses support that common frogs persisted in a large sanctuary (*sensu* Recuero & García-París 2011) encompassing northern Iberia (Figs. 1, 5). Furthermore, their genetic diversity and structure across the area confirms separate microrefugia (Fig. 1), which likely expanded during the cold glacial cycles, but probably contracted during the warm interglacials (Figs. 4–5). The accuracy of the projected distributions is obviously bounded by SDM performance in capturing the complex ecological conditions that define species' preferences (notably microhabitats), and bioclimatic reconstructions are only informative of the latest stages of the Pleistocene (i. e. not when the lineages initially diverged). Here, glacial instead of post-glacial expansions coincide with the expectations for *R. temporaria*, an ecologically versatile species often associated to the Euro-Siberian realm (*sensu* De Lattin 1957; Schmitt & Varga 2012), and one of the most

cold-tolerant amphibians of temperate Europe, both at the larval (Gutiérrez-Pesquera et al. 2017) and terrestrial stages (critical thermal minimum as low as -2.4°C, AGN unpublished data).

Is the Iberian sanctuary of common frogs a hotspot of cryptic speciation and/or of cyto-nuclear discordances? From our genomic analyses, the answer is both. Within our study area, three of the four deeply-diverged mitochondrial clades (Vences et al. 2013, 2017) correspond to significant nuclear clusters. In particular, we recovered the nuclear identity of the Galician and Asturian populations (T1 and T2), tentatively attributed to the subspecies *R. temporaria parvipalmata* following previous allozyme and mitochondrial analyses (Arano et al. 1993, Veith et al. 2002, 2012). Given its early nuclear divergence and narrow transition with the eastern clade (*R. temporaria temporaria*), this taxon might actually represent yet another cryptic event of amphibian speciation revealed by genomic phylogeography.

First, the dated split (2.3–6.2Mya) between *R. t. temporaria* and *R. t. parvipalmata* falls within the timeframe reported for other cryptic species of amphibians (3–6My; Dufresnes et al. 2019a, 2019b, 2020, and references therein). Second, the hybrid zone is remarkably narrow (25km), despite presumably weak or absent geographical barriers to dispersal in the area. Rivers in the lowlands (e. g. Deva-Cares, Nansa), and the rarity of ponds in the limestone highlands, may locally reduce connectivity across the transition zone, but similar landscapes are found within the ranges of each lineage, without causing deep genetic structure among populations (File S6). Such a steep transition therefore probably indicates reproductive isolation. Under a tension zone model mediated by heterozygote disadvantage, selection against hybrids corresponds to the fitness difference $s^*$ between the center and the edge of the hybrid zone, and can be approximated from the cline width $w$ and dispersal $\sigma$, as $w \approx 2\sigma / \sqrt{s^*}$ (Barton & Gale 1993). Assuming a dispersal rate of 0.4km/year (Smith & Green 2005, Dolmen & Seland 2016), and a generation time of 8 years (calculated from an average sexual maturity and lifespan of 3 and 6 years, respectively; Gibbons & McCarthy 1984, Ryser 1988, Miaud et al. 1999), $\sigma$ = 3.2 km/generation and $w$ = 25 km (CI: 18.2–38.9 km) give $s^*$ = 0.07 (CI: 0.03–0.12) for this hybrid system. While selection is usually stronger in hybrid zones involving genetically and eco-morphologically more diverged species (e. g. $s^*$ = 0.21 in *Bombina bombina*/*variegata*, reviewed in Barton & Gale 1993), the majority of transitions between cryptic European anurans actually features lower selection against hybrids, e. g. $s^*$ = 0.03 for *Pelobates fuscus*/*vespertinus* (Dufresnes et al. 2019a); $s^*$ = 0.05 for *Hyla arborea*/*orientalis* (computed from Dufresnes et al. 2015). In Spanish common frogs, F1 hybrids obtained from a few artificial crosses between adults collected at our localities 10 (T2) and 25 (T6) did not display particularly high mortality rates during larval development (Palomar et al. 2017, 2019). Post-zygotic incompatibilities could however

affect their fertility, and be more predominantly expressed in backcrosses, after recombination has generated Dobzhansky-Muller incompatibilities, causing hybrid breakdown (Orr 1995).

Our genomic analyses thus contrast with previous allozyme data, which inferred introgression over hundreds of kilometers (Veith et al. 2002, 2012). At the transition, whether the westward shift of mitochondrial compared to nuclear alleles reflects pre- (assortative mating) or post-zygotic isolation (asymmetric incompatibilities) *vs* demographic processes (e. g. range shifts and sex-biased dispersal) remains an open question. For instance, this pattern is consistent with higher fitness of ♂ T2 × ♀ T6 crosses compared to the reciprocal direction, but could also have arisen following an eastward invasion of T2 with male-biased dispersal, or a westward invasion of T6 with female-biased dispersal, since both lineages show signs of population expansions (Fig. 4). According to genetic data, dispersal is supposedly female-biased in *R. temporaria* (Palo et al. 2004). These hypotheses could be tested by integrating analyses of hybrid zone movement (Wielstra 2019), controlled experimental crosses, and direct assessment of sex-specific dispersal patterns (e. g. through capture-mark-recapture techniques).

From the two lines of evidence, and in accordance with previous studies on anuran speciation, we therefore hypothesize that two incipient species of common frogs can be distinguished. The European Common Frog *R. temporaria* Linnaeus, 1758 occupies most of Europe, including northeastern Spain, corresponding to lineages T3-T6. The Galician Common Frog *R. parvipalmata* López-Seoane, 1885 is endemic to northwestern Spain, corresponding to lineages T1-T2. The nomen *parvipalmata*, described from Galicia (type locality attributed to "La Coruña", belonging to lineage T1) is accordingly the oldest available for the western clade (Frost 2019). Although our analyses insufficiently cover the nuclear transition between T1 and T2 (Fig. 1), these unlikely represent additional speciation events given the comparatively lower divergence (~2My), and should therefore not necessitate further taxonomic changes.

Morphologically, the two species recognized here are not necessarily cryptic: frogs belonging to *R. parvipalmata* have been documented to exhibit reduced feet webbing and a lower number of pulses per call compared to other populations assigned to *R. temporaria* (Vences 1992), although these specificities only apply to the westernmost Galician populations (where frogs are smaller). Understanding whether these traits reflect local adaptation to different ecological conditions (but see the overlapping projections in Fig. 5) and/or are involved in the partial reproductive isolation between the two species will require new phenotypic and habitat assessments. The ecological requirements of these species are presumably similar in northern Spain (File S10), and the differences highlighted by the bioclimatic models might stem from the range extents – *R. parvipalmata* is restricted to a small geographic region (<50,000km$^2$), while *R.*

*temporaria* inhabits vast areas (>8 million km$^2$) and thus occupies a much broader realized niche overall (File S10).

This first result thus adds to a growing body of literature supporting that diverging lineages persisting in separate microrefugia can be on the path to speciation, despite occasional gene flow during secondary contacts (e. g. Díaz-Rodríguez et al. 2017, Dufresnes et al. 2018). For the cold-tolerant *Rana* frogs, this outcome is remarkable because Spanish populations expanded and thrived during the prolonged glacials rather than during the short interglacial cycles only (Figs. 4-5; see also Galán et al. 2010 for the Galician populations of *R. parvipalmata*), thus experiencing longer opportunities for lineage fusion compared to species with Mediterranean affinities. Such ecological flexibility is today reflected in the high levels of genetic variation in *R. temporaria* range wide (Vences et al. 2013), and by a complex history of divergences and subsequent fusions of lineages in some regions (Marchesini et al. 2017, see next section). Finally, it is worth noting that the phylogeography of Spanish common frogs shows similar patterns of west-east fragmentation to those reported in other Iberian amphibians associated with the Atlantic region, including *Salamandra salamandra* (García-París et al. 2003), *Lissotriton helveticus* (Recuero & García-París 2011), *Ichthyosaura alpestris* (Recuero et al. 2014), and *Alytes obstetricans* (Maia-Carvalho et al. 2018), which are thus good candidates for cryptic speciation events as well.

*Ghost mitochondrial lineages in* R. temporaria

The most divergent mitochondrial clade sampled in northern Spain (T6) forms a single, homogeneous nuclear cluster with the widespread T4 mtDNA lineage in all analyses (Figs. 1-2, File S3d). The origin of this ghost T6 mtDNA lineage is puzzling. Contrarily to Phuong et al. (2017), here we did not find significant associations between patterns of cyto-nuclear discordances or genetic diversity and the variability of environmental conditions during the late-Pleistocene, perhaps because the ranges remained broadly suitable for this species during the last glaciation (Fig. 5, File S8). Hence, we rather envisage two alternative scenarios: (1) mitochondrial capture from a now-extinct nuclear T6 cluster; or (2) *de novo* emergence of the T6 mtDNA by drift and/or selection.

The first hypothesis is consistent with the biogeography of the Cantabrian Range, which hosts endemic refugial clades in other amphibians with a broad European distribution (e. g. Recuero & García-París 2011). The T6 evolutionary lineage could have thus arisen in *R. temporaria* during the Pleistocene, and then merged with T4 until complete fusion (as seen among Alpine lineages, Marchesini et al. 2017),

to the point that only its mitochondrial legacy remains. Subsequent glacial expansions (Fig. 4) would have then spread T6 mtDNA in most of Cantabria and the west of the Basque Country.

Alternatively, the second hypothesis that T6 recently derived from the T4 cluster is consistent with the homogenous nuclear diversity and pattern of isolation-by-distance. In this case, the rise and maintenance of T6 would simply stem from the lower effective size of mtDNA, eventually promoted by male-biased dispersal (but see Palo et al. 2004). Our SDMs indicate a minor role for climatic niche differences in maintaining the T6 and T4 mtDNA lineages apart (File S8b), but analyses of complete mitogenomes could inform on whether selection played a role in accelerating the divergence (e. g. Bernardo et al. 2019).

While advocating our hypothesis that subdivided refugia can be hotspots for cyto-nuclear discordances (although not necessarily due to climatic instability), the T6 ghost lineage exemplifies how mitochondrial phylogeographies may dramatically distort our perception of the evolutionary history, diversity and systematics of species complexes (Zink & Barrowclough 2008, Hinojosa et al. 2019). Deep mitochondrial lineages without signs of nuclear differentiation are increasingly reported in the literature (e. g. Irwin 2002, Bernardo et al. 2019). For instance, the mitogroups identified by Bernardo et al. (2019) in Californian lizards were estimated at about ~5My, an age mimicking many species-level divergences in Palearctic amphibians (Ehl et al. 2019, Dufresnes et al. 2020). In *R. temporaria*, future surveys should focus on T3, another enigmatic mtDNA lineage restricted to a single valley (Benasque) in the Central Pyrenees (Vences et al. 2017). Diverged but ephemeral mtDNAs also persist in other Iberian taxa, e. g. the Pyrenean haplogroup E of *Alytes obstetricans* (Maia-Carvalho et al. 2018). Hence, the maintenance of ghost mitochondrial lineages can create mirages of cryptic species (Hinojosa et al. 2019), but at the same time mitochondrial capture and replacement may conceal genuine evolutionary divergences (Dufresnes et al. 2019b). Because these two phenomena might be more common than previously assumed (Dufresnes et al. 2019b), we recommend that taxonomic revisions involving taxa from refugial areas should be based on genomic evidence to make decisions on species-level divergence (Suchan et al. 2017).

The same rationale applies when interpreting biological results from model organisms under a phylogeographic framework. Because of its abundance and broad ecological niche, its wide geographic and altitudinal distribution, as well as its strong genomic and phenotypic plasticity, the common frog has been a model system to address fundamental topics in ecological, evolutionary, and conservation sciences, e. g. local adaptation (e.g. Miur et al. 2014), dispersal (e. g. Palo et al. 2004, Dolmen & Seland 2016), epidemiology (e. g. Duffus et al. 2019), resistance to abiotic stresses (e.g. Marquis et al. 2008), sex

determination mechanisms (e. g. Rodrigues et al. 2016), or sex-chromosome evolution (e. g. Rodrigues et al. 2018). The present survey thus provides the necessary context to carry out more comprehensive studies on Iberian common frogs, where the overlooked diversity offers a promising playground for future research.

*Conclusions*

The genomic phylogeography of common frogs across their refugial range in northern Spain distinguished the Galician/Asturian endemic *Rana parvipalmata* as a new species of vertebrate for Europe, while the eastern Cantabrian populations of *R. temporaria* fixed a ghost, deeply-diverged mtDNA lineage. These patterns support that refugia within refugia are both hotspots of cryptic speciation and of extreme cyto-nuclear discordances, and imply that their prevalence has been either under- or over-estimated by mitochondrial phylogeographies, depending on whether the dynamics of allopatric divergence *vs* gene flow during the Pleistocene restricted admixture, or promoted range-wide introgression between lineages.

**Acknowledgements**

We thank C. Cabido, I. Garin, A. Gosá, F. Martínez, J. Rubines, X. Rubio, and G. Sánchez-Montes for help in sample collection. This study was funded by the Swiss National Science Foundation (fellowship P2LAP3_171818 to CD, and grant 31003A_166323 to NP). MV was supported by the Deutsche Forschungsgemeinschaft (grant VE247/16-1 – HO 3492/6-1) in the framework of the 'TaxonOmics' priority program, SNL by the RFBR (grant 20-04-00918), and AGN by the Spanish Ministry of Science, Innovation and Universities (MICINN grants CGL2012-40246 and CGL2017-86924-P).

**References**

Arano B, Esteban M, Herrero P. 1993. Evolutionary divergence of the Iberian brown frogs. Annales des Sciences Naturelles - Zoologie et Biologie Animale, 14: 49-57.

Avise J. 2000. Phylogeography: The history and formation of species. Cambridge, MA: Harvard University Press.

560 Barton N, Gale KS. 1993. Genetic analysis of hybrid zones. Pp 13-45 in: Hybrid zones and the
561 evolutionary process (R. Harrison, Ed.). New York: Oxford University Press.

562 Bernardo PH, Sánchez-Ramírez S, S Sánchez-Pacheco, ST Álvarez-Castañeda, EF Aguilera-Miller, FR
563 Mendez-de la Cruz, RW Murphy. 2019. Extreme mito-nuclear discordance in a peninsular lizard:
564 the role of drift, selection, and climate. Heredity 123, 359-370.

565 Bonnet T, Leblois R, Rousset F, Crochet P-A. 2017. A reassessment of explanations for discordant
566 introgressions of mitochondrial and nuclear genomes. Evolution, 71, 2140–2218.

567 Bouckaert R, Heled K, Khünert D, Vaughan T, Wu CH, Xie D, Suchard MA, Rambaut A, Drummond AJ.
568 2014. BEAST 2: a software platform for Bayesian Evolutionary Analysis. PLoS Computational
569 Biology 10, e1003537.

570 Bouckaert RR & Drummond AJ. 2014. DensiTree 2: seeing trees through the forest.
571 https://doi.org/10.1101/012401.

572 Bouckaert RR, Drummond AJ. 2017. bModelTest: Bayesian phylogenetic site model averaging and model
573 comparison. BMC Evolutionary Biology, 17, 42.

574 Brelsford A, Dufresnes C, Perrin N. 2016. High-density sex-specific linkage maps of a European tree frog
575 (*Hyla arborea*) identify the sex chromosome without information on offspring sex. Heredity 116,
576 177–181.

577 Brelsford A, Lavanchy G, Sermier R, Rausch A, Perrin N. Identifying homomorphic sex chromosomes
578 from wild-caught adults with limited genomic resources. Molecular Ecology Resources 17, 752-
579 759.

580 Cahill JA, Green RE, Fulton TL, Stiller M, Jay F, Ovsyanikov N, Salamzade R, St John J, Stirling I,
581 Slatkin M, Shapiro B. 2013. Genomic evidence for island population conversion resolves
582 conflicting theories of polar bear evolution. PLoS Genetics 9, e1003345.

583 Canestrelli D, Bisconti R, Sacco F, Nascetti G. 2014. What triggers the rising of an intraspecific
584 biodiversity hotspot? Hints from the agile frog. Scientific Reports 4, 5042.

585 Catchen J, Hohenlohe P, Bassham S, Amores A, Cresko W. 2013. Stacks: an analysis tool set for
586 population genomics. Molecular Ecology, 22, 3124–3140.

587 Chan KM, Levin SA, 2005. Leaky prezygotic isolation and porous genomes: rapid introgression of
588 maternally inherited DNA. Evolution, 59, 720–729.

589 Chenuil A, Cahill AE, Délémontey N, Du Salliant E, Fanton H. 2019. Problems and questions posed by
590 cryptic species. A framework to guide future studies. Pp 77-106 in: *From Assessing to Conserving*
591 *Biodiversity. History, Philosophy and Theory of the Life Sciences, vol 24* (eds Casetta E, Marques
592 da Silva J, Vecchi D). Springer, Cham.

593 Collins RA, Cruickshank RH. 2012. The seven deadly sins of DNA barcoding. Molecular Ecology
594 Resources, 13, 969–975.

595 Currat M, Ruedi M, Petit RJ, Excoffier L. 2008. The hidden side of invasions: Massive introgression by
596 local genes. Evolution, 62, 1908–1920.

597 Dai C, Wang W, Lei F. 2013. Multilocus phylogeography (mitochondrial, autosomal and Z-chromosomal
598 loci) and genetic consequences of long-distance male dispersal in Black-throated tits (*Aegithalos*
599 *concinnus*). Heredity 110, 457–465.

600 De Lattin G. 1957. Die Ausbreitungszentren der holarktischen Landtierwelt. In: Verhandlungen der
601 Deutschen Zoologischen Gesellschaft vom 21. bis 26. Mai 1956 in Hamburg. Edited by Pflugfelder
602 O. Geest & Portig, Leipzig, pp. 380–410.

603 Derryberry EP, Derryberry GE, Maley JM, Brumfield RT. 2014. HZAR: hybrid zone analysis using an R
604 software package. Molecular Ecology Resources 14, 652-663.

605 Díaz-Rodríguez J, Gehara M, Marquez R, Vences M, Goncalves H, Sequeira F, Martínez-Solano I, Tejedo
606 M. 2017. Integration of molecular, bioacoustical and morphological data reveals two new cryptic
607 species of *Pelodytes* (Anura, Pelodytidae) from the Iberian Peninsula. Zootaxa, 4243, 1–41.

608 Dolmen D, Seland J. 2016. How fast do amphibians disperse? Introductions, distribution and dispersal of
609 the common frog (*Rana temporaria*) and the common toad (*Bufo bufo*) on a coastal island in
610 Central Norway. Fauna norvegica 36: 33-46.

611 Dubey S, Maddelena T, Bonny L, Jeffries DL, Dufresnes C. 2019. Population genomics of an exceptional
612 hybridogenetic system of *Pelophylax* water frogs. BMC Evolutionary Biology, 19, 164.

613 Duffus ALJ, Garner TWJ, Nichols RA, Standridge J, Earl JE. 2019. Modelling Ranavirus transmission in
614 populations of common frogs (*Rana temporaria*) in the United Kingdom. Viruses, 11, 556.

615 Dufresnes C, Litvinchuk SN, Leuenberger J, Ghali K, Zinenko O, Stöck M, Perrin N. 2016. Evolutionary
616 melting pots: a biodiversity hotspot shaped by ring diversifications around the Black Sea in the
617 Eastern tree frog (*Hyla orientalis*). Molecular Ecology 25, 4285–4300.

618 Dufresnes C, Mazepa G, Rodrigues N, Brelsford A, Litvinchuk SN, Sermier R, Lavanchy G, Betto-
619 Colliard C, Blaser O, Borzée A, Cavoto E, Fabre G, Ghali K, Grossen C, Horn A, Leuenberger J,
620 Phillips BC, Saunders PA, Savary R, Maddalena T, Stöck M, Dubey S, Canestrelli D, Jeffries DL.
621 2018. Genomic evidence for cryptic speciation in tree frogs from the Apennine Peninsula, with
622 description of *Hyla perrini* sp. nov. Frontiers Ecology & Evolution 6, 144.

623 Dufresnes C, Strachinis I, Suriadna N, Mykytynets G, Cogălniceanu D, Vukov T, Székely P, Vukov T,
624 Arntzen JW, Wielstra B, Lymberakis P, Geffen E, Gafny S, Kumlutaş Y, Ilgaz C, Candan K, Mizsei
625 E, Szabolcs M, Kolenda K, Smirnov N, Géniez P, Lukanov S, Crochet P-A, Dubey S, Perrin N,
626 Litvinchuk SN, Denoël M. 2019a. Phylogeography of a cryptic speciation continuum in Eurasian
627 spadefoot toads (*Pelobates*). Molecular Ecology, 28, 3257–3270.

628 Dufresnes C, Mazepa G, Jablonski D, Caliari Oliveira R, Wenseleers T, Shabanov DA, Auer M, Ernst R,
629 Koch C, Ramírez-Chaves HE, Mulder KP, Simonov E, Tiutenko A, Kryvokhyzha D, Wennekes PL,
630 Zinenko OI, Korshunov OV, Al-Johany AM, Peregontsev EA, Masroor R, Betto-Colliard C, Denoël
631 M, Borkin LJ, Skorinov DV, Pasynkova RA, Mazanaeva LF, Rosanov JM, Dubey S, Litvinchuk
632 SN. 2019b. Fifteen shades of green: the evolution of *Bufotes* toads revisited. Molecular
633 Phylogenetics Evolutionary. Molecular Phylogenetics & Evolution, 141, 106615.

634 Dufresnes C, Pribille M, Alard B, Gonçalves H, Amat F, Crochet P-A, Dubey S, Perrin N, Fumagalli L,
635 Vences M, Martínez-Solano I. 2020. Integrating hybrid zone analyses in species delimitation:
636 lessons from two anuran radiations of the Western Mediterranean. Heredity.
637 https://doi.org/10.1038/s41437-020-0294-z.

638 Dufresnes C. 2019. Phylogeography and hybrid zones of Palearctic amphibians. NCBI SRA. Retrieved
639 from https://www.ncbi.nlm.nih.gov/bioproject/542138.

640 Ehl S, Vences M, Veith M. 2019. Reconstructing evolution at the community level: a case study on
641 Mediterranean amphibians. Molecular Phylogenetics & Evolution 134, 211-225.

642 Elith J, Graham CH, Anderson RP, Dudík M, Ferrier S, Guisan A, Hijmans RJ, Huettmann F, Leathwick
643 JR, Lehmann A, Li J, Lohmann G, Loiselle BA, Manion G, Moritz G, Nakamura M, Nakazawa Y,
644 Overton JM, Peterson AT, Phillips SJ, Richardson K, Scachetti-Pereira R, Schapire RE, Soberón J,

Williams S, Wisz MS, Zimmermann NE. 2006: Novel methods improve prediction of species' distributions from occurrence data. Ecography, 29, 129–151

Excoffier L, Foll M, Petit RJ. 2009. Genetic consequences of range expansions. Annual Review of Ecology, Evolution, and Systematics, 40, 481–501.

Frost D. 2019. Amphibian Species of the World: an Online Reference. Version 6.0. American Museum of Natural History, New York, USA (accessed September 10th 2019). http://research.amnh.org/herpetology/amphibia/index.html.

Galán P, Ludewig A-K, Kmiec J, Hauswaldt S, Cabana M, Ferreiro R, Vences M. 2010. Low mitochondrial divergence of rediscovered southern relict populations of *Rana temporaria parvipalmata* in Spain. Amphibia-Reptilia, 31, 144-148.

García-París M, Alcobendas M, Buckley D, Wake D. 2003. Dispersal of viviparity across contact zones in Iberian populations of fire salamanders (*Salamandra*) inferred from discordance of genetic and morphological traits. Evolution 57, 129–143.

Garrick RC, Banusiewicz JD, Burgess S, Hyseni C, Symula RE. 2019. Extending phylogeography to account for lineage fusion. Journal of Biogeography 46, 268-278.

Gibbons MM, McCarthy TK. 1984. Growth, maturation and survival of frogs *Rana temporaria* L. Holarctic Ecology, 7, 419-427.

Gómez A, Lunt DH. 2007. Refugia within refugia: patterns of phylogeographic concordance in the Iberian Peninsula. Pp. 155-188 in: *Phylogeography of Southern European Refugia* (eds Weiss S, Ferrand N). Springer, Amsterdam, Netherlands.

Gouy M, Guindon S, Gascuel O. 2010. SeaView version 4: A multiplatform graphical user interface for sequence alignment and phylogenetic tree building. Molecular Biology & Evolution. 27, 221-224.

Guidon S, Dufayard JF, Lefort V, Anisimova M, Hordijk W, Gascuel O. 2010. New algorithms and methods to estimate maximum-likelihood phylogenies: assessing the performance of PhyML 3.0. Systematic Biology 59, 307–321.

Gutiérrez-Pesquera LM, Tejedo M, Olalla-Tárraga MÁ, Duarte H, Nicieza A, Solé M. 2016. Testing the climate variability hypothesis in thermal tolerance limits of tropical and temperate tadpoles. Journal of Biogeography, 43, 1166–1178.

673 Gutiérrez-Rodríguez J, Barbosa AM, Martínez-Solano I. 2017a. Integrative inference of population history
674 in the Ibero-Maghrebian endemic *Pleurodeles waltl* (Salamandridae). Molecular Phylogenetics and
675 Evolution 112: 122-137.

676 Gutiérrez-Rodríguez J, Barbosa AM, Martínez-Solano I. 2017b. Present and past climatic effects on the
677 current distribution and genetic diversity of the Iberian Spadefoot toad (*Pelobates cultripes*): an
678 integrative approach. Journal of Biogeography 44: 245-258.

679 Heled J, Drummond AJ. 2008. Bayesian inference of population size history from multiple loci. BMC
680 Evolutionary Biology, 8, 289.

681 Heller R, Chikhi L, Siegismund HR. 2013. The confounding effect of population structure on Bayesian
682 skyline plot inferences of demographic history. PLoS ONE 8, e62992.

683 Hewitt GM. 1996. Some genetic consequences of ice ages, and their role in divergence and speciation.
684 Biological Journal of the Linnean Society, 58, 247-276.

685 Hinojosa JC, Koubínová D, Szenteczki MA, Pitteloud C, Dincă V, Alvarez N, Vila R. A mirage of cryptic
686 species: Genomics uncover striking mitonuclear discordance in the butterfly *Thymelicus sylvestris*.
687 Molecular Ecology 28, 3857-3868.

688 Irwin DE. 2002. Phylogeographic breaks without geographic barriers to gene flow. Evolution 26, 2383-
689 2394.

690 Jombart T. 2008. adegenet: a R package for the multivariate analysis of genetic markers. Bioinformatics
691 24, 1403–1405.

692 Jörger KM, Schrödl M. 2013. How to describe a cryptic species? Practical challenges of molecular
693 taxonomy. Frontiers in Zoology 10, 59.

694 Krishnamurthy KP, Francis RA. 2012. A critical review on the utility of DNA barcoding in biodiversity
695 conservation. Biodiversity & Conservation, 21, 1901–1919.

696 Lefort V, Longueville JE, Gascuel O. 2017. SMS: Smart Model Selection in PhyML. Molecular Biology
697 & Evolution 34, 2422–2424.

698 Lobo JM, Martínez-Solano Í, Sanchiz B. 2016. A review of the palaeoclimatic inference potential of
699 Iberian Quaternary fossil batrachians. Palaeobiodiversity and Palaeoenvironments, 96, 125–148.

Maia-Carvalho B, Gomes-Vale C, Sequeira F, Ferrand N, Martínez-Solano I, Gonçalves H. 2018. The roles of allopatric fragmentation and niche divergence in intraspecific lineage diversification in the common midwife toad (*Alytes obstetricans*). Journal of Biogeography, 45, 21–46.

Marchesini A, Ficetola GF, Cornetti L, Battisti A, Vemesi C. 2017. Fine-scale phylogeography of *Rana temporaria* (Anura: Ranidae) in a putative secondary contact zone in the southern Alps. Biological Journal of the Linnean Society, 122, 824–837.

Marquis O, Miaud C, Lena J-P. 2008. Developmental responses to UV-B radiation in common frog *Rana temporaria* embryos from along an altitudinal gradient. Population Ecology, 50, 123-130.

Miaud C, Guyétant R, Elmberg J. 1999. Variations in life-history traits in the common frog *Rana temporaria* (Amphibia: Anura): a literature review and new data from the French Alps. Journal of Zoology, 249, 61-73.

Miur AP, Biek R, Thomas R, Mable BK. 2014. Local adaptation with high gene flow: temperature parameters drive adaptation to altitude in the common frog (*Rana temporaria*). Molecular Ecology 23, 561-574.

Morgan-Richards M, Bulgarella M, Sivyer L, Dowle EJ, Hale M, McKean NE, Trewick SA. 2017. Explaining large mitochondrial sequence differences within a population sample. Royal Society Open Science, 4, 170730.

Orr H. 1995. The population genetics of speciation: the evolution of hybrid incompatibilities. Genetics, 139, 1805–1813.

Palomar G, Ahmad F, Vasemägi A, Matsuba C, Nicieza AG, Cano JM. 2017. Comparative high-density linkage mapping reveals conserved genome structure but variation in levels of heterochiasmy and location of recombination cold spots in the common frog. G3 (Bethesda), 7, 637–645

Palomar G, Vasemägi A, Ahmad F, Nicieza AG, Cano JM. 2019. Mapping of quantitative trait loci for life history traits segregating within common frog populations. Heredity, 122, 800–808.

Pavlova A, Amos JN, Joseph L, Loynes K, Austin JJ, Keogh JS, Stone GN, Nicholls JA, Sunnucks P. 2013. Perched at the mito-nuclear crossroads: Divergent mitochondrial lineages correlate with environment in the face of ongoing nuclear gene flow in an Australian bird. Evolution, 67, 3412-3428.

728 Petit R, Aguinagalde I, de Beaulieu JL, Bittkau C, Brewer S, Cheddadi R, Ennos R, Fineschi S, Grivet D,
729 Lascoux M, Mohanty A, Müller-Starck G, Demesure-Musch B, Palmé A, Martín JP, Rendell S,
730 Vendramin GG. 2003. Glacial refugia: hotspots but not melting pots of genetic diversity. Science
731 300, 1563-5.

732 Phillips S, Anderson R, Schapire R. 2006. Maximum entropy modeling of species geographic
733 distributions. Ecological Modeling 190, 231–259.

734 Phillips SJ, Dudík M. 2008. Modeling of species distributions with Maxent: new extensions and a
735 comprehensive evaluation. Ecography 31, 161–175.

736 Phuong MA, Bi K, Moritz C. 2017. Range instability leads to cytonuclear discordance in a
737 morphologically cryptic ground squirrel species complex. Molecular Ecology, 26, 4743–4755.

738 Provan J, Bennett KD. 2008. Phylogeographic insights into cryptic glacial refugia. Trends in Ecology &
739 Evolution, 21, 564-71.

740 Recuero E, García-París M. 2011. Evolutionary history of *Lissotriton helveticus*: multilocus assessment of
741 ancestral vs. recent colonization of the Iberian Peninsula. Molecular Phylogenetics and Evolution,
742 60, 170-182.

743 Recuero E, Buckley D, García-París M, Arntzen JW, Cogălniceanu D, Martínez-Solano I. 2014.
744 Evolutionary history of *Ichthyosaura alpestris* (Caudata, Salamandridae) inferred from the
745 combined analysis of nuclear and mitochondrial markers. Molecular Phylogenetics and Evolution
746 81, 207-220.

747 Rodrigues N, Vuille Y, Brelsford A, Merilä J, Perrin N. 2016. The genetic contribution to sex
748 determination and number of sex chromosomes vary among populations of common frogs (*Rana*
749 *temporaria*). Heredity 117, 25-32.

750 Rodrigues N, Studer T, Dufresnes C, Perrin N. 2018. Sex-chromosome recombination in common frogs
751 brings water to the Fountain-of-Youth. Molecular Biology & Evolution, 35, 1821.

752 Rosenberg NA. 2003. The shapes of neutral gene genealogies in two species: Probabilities of monophyly,
753 paraphyly, and polyphyly in a coalescent model. Evolution, 57, 1465–1477.

754 Ryser J. 1988. Determination of growth and maturation in the common frog, *Rana temporaria*, by
755 skeletochronology. Journal of Zoology, 216, 673–685.

Sánchez-Montes G, Recuero E, Barbosa AM, Martínez-Solano I. 2019. Complementing the Pleistocene biogeography of European amphibians: testimony from a southern Atlantic species. Journal of Biogeography, 46, 568-583.

Schmitt T. 2007. Molecular biogeography of Europe: Pleistocene cycles and postglacial trends. Frontiers in Zoology, 4, 11.

Schmitt T, Varga Z. 2012. Extra-Mediterranean refugia: The rule and not the exception? Frontiers in Zoology, 9, 22.

Smith MA, Green DM. 2005. Dispersal and the metapopulation paradigm in amphibian ecology and conservation: are all amphibian populations metapopulations? Ecography 28, 110–128.

Struck TH, Feder JL, Bendiksby M, Birkeland S, Cerca J, Gusarov VI, Kistenich S, Larsson KH, Liow LH, Nowak MD, Stedje B, Bachmann L, Dimitrov D. 2018. Finding evolutionary processes hidden in cryptic species. Trends Ecol Evol. 33, 153–163.

Stuart JR, Lister AM, Barnes I, Dale L. 2009. Refugia revisited: individualistic responses of species in space and time. Proceedings of the Royal Society B, 277, 661–671.

Suchan T, Espíndola A, Rutschmann S, Emerson BC, Gori K, Dessimoz C, Arrigo N, Ronikier M, Alvarez N. 2017. Assessing the potential of RAD-sequencing to resolve phylogenetic relationships within species radiations: The fly genus *Chiastocheta* (Diptera: Anthomyiidae) as a case study. Molecular Phylogenetics & Evolution, 114, 189–198.

Swets JA. 1988. Measuring the accuracy of diagnostic systems. Science 240, 1285–1293.

Toews DPL, Brelsford A. 2012. The biogeography of mitochondrial and nuclear discordance in animals. Molecular Ecolgy 21, 3907–3930.

Veith M, Vences M, Vieites DR, Nieto-Roman S, Palanca-Soler A. 2002. Genetic differentiation and population structure within Spanish common frogs (*Rana temporaria* complex; Ranidae, Amphibia). Folia Zoologica. Prague, 51, 307–318.

Veith M, Baumgart A, Dubois A, Ohler A, Galán P, Vieites DR, Nieto-Román S, Vences M. 2012. Discordant patterns of nuclear and mitochondrial introgression in Iberian populations of the European common frog (*Rana temporaria*). Journal of Heredity, 103, 240–249.

783 Vences M. 1992. Zur Biologie der nordwestspanischen Braunfrösche *Rana iberica* Boulenger, 1879 und
784 *Rana temporaria parvipalmata* Seosane, 1885. Salamandra, 28, 61-71.

785 Vences M, Grossenbacher K, Puente M, Palanca A, Vieites DR. 2003. The Cambalès fairy tale:
786 elevational limits of *Rana temporaria* (Amphibia: Ranidae) and other European amphibians
787 revisited. Folia Zoologica, 52, 189–202.

788 Vences M, Hauswaldt JS, Steinfartz S, Rupp O, Goesmann A, Künzel S, Orozco-terWengel P, Vieites
789 DR, Nieto-Roman S, Haas S, Laugsch C, Gehara M, Bruchmann S, Pabijan M, Ludewig AK,
790 Rudert D, Angelini C, Borkin LJ, Crochet PA, Crottini A, Dubois A, Ficetola GF, Galán P, Geniez
791 P, Hachtel M, Jovanovic O, Litvinchuk SN, Lymberakis P, Ohler A, Smirnov NA. 2013. Radically
792 different phylogeographies and patterns of genetic variation in two European brown frogs, genus
793 *Rana*. Molecular Phylogenetics and Evolution, 68, 657-670.

794 Vences M, Sarasola-Puente V, Sanchez E, Amat F, Hauswaldt JS. 2017. Diversity and distribution of deep
795 mitochondrial lineages of the common frog, *Rana temporaria*, in northern Spain. Salamandra 53,
796 25-33.

797 Warren DL, Glor RE, Turelli M. 2010. ENMTOOLS: a toolbox for comparative studies of environmental
798 niche models. Ecography, 33, 607–611.

799 Watanabe S, Hajima T, Sudo K, Nagashima T, Takemura H, Okajima H, Nozawa T, Kawase H, Abe M,
800 Yokohata T, Ise T, Sato H, Kato E, Takata K, Emori S, Kawamiya M. 2011. MIROC-ESM 2010:
801 model description and basic results of CMIP5-20c3 m experiments. Geoscientific Model
802 Development 4, 845–872.

803 Web of Knowledge (2019). https://apps.webofknowledge.com/. Consulted September 10th 2019.

804 Wielstra B. 2019. Historical hybrid zone movement: more pervasive than appreciated. Journal of
805 Biogeography 46, 1300–1305.

806 Yuan ZY, Zhou WW, Chen X, Poyarkov NA Jr, Chen HM, Jang-Liaw NH, Chou WH, Matzke NJ, Iizuka
807 K, Min MS, Kuzmin SL, Zhang YP, Cannatella DC, Hillis DM, Che J. 2016. Spatiotemporal
808 Diversification of the true frogs (Genus *Rana*): a historical framework for a widely studied group of
809 model organisms. Systematic Biology, 65, 824-842.

810 Zink RM, Barrowclough G. 2008. Mitochondrial DNA under siege in avian phylogeography. Molecular
811 Ecology 17, 2107–2121.

## Data Accessibility

Sequences included in the main mitochondrial phylogeny are available from Vences et al. (2017), and the mtDNA barcoding information is provided in File S1. The nuclear sequences (individual raw sequence reads) are archived in the NCBI SRA under bioproject PRJNA542138 (Dufresnes 2019).

## Author contributions

Designed the study: CD, AGN, MV, NP, IMS; conducted fieldwork: CD, AGN, NR, IMS; conducted labwork: CD; conducted analyses: CD, SNL, DLJ; wrote the manuscript: CD, assisted by all co-authors.

## Figures

**Fig. 1:** (A) Simplified mitochondrial phylogeny based on 4.3kb (see File S3b for the full tree) and distribution of the major mtDNA lineages in N-Iberia, barcoded using the diagnostic *cyt-b* (see File S3b). (B) Simplified nuclear phylogeny based on ~142kb of RAD tags (see File S3d for the full tree), individual ancestries as assigned by STRUCTURE (barplots) and the corresponding population ancestries to the three clusters identified (map). Grey levels show topography. Photo credit: CD.

**Fig. 2:** PCA on individual nuclear allele frequencies. Each dot corresponds to an individual, colored by its mtDNA lineage (labelled). The first axis distinguishes the two species, and emphasizes that most hybrid specimens bear *R. temporaria* mtDNA. The second axis reflects intraspecific structure within *R. parvipalmata* (T1 *vs* T2).

**Fig. 3:** Cline fitting on mitochondrial allele frequencies (T6, dash line) and nuclear genomic average ancestry (STRUCTURE's Q to *R. temporaria*, plain line) along a west-east transect in northern Spain (localities 11–28). The grey areas show the 95% confidence intervals of the clines. For the nuclear data, the observed frequencies are displayed by crosses and circles, the latter reflecting relative sample sizes.

**Fig. 4:** Distribution of the genetic diversity of common frogs in N-Iberia: (A) for 501bp of the mitochondrial *cyt-b* (nucleotide diversity $\pi$); (B) for 566 nuclear SNPs (observed heterozygosity $H_o$). (C) Demographic analysis (EBSP) of the well-sampled clades T2 (*R. parvipalmata*) and T6+T4 (*R. temporaria*), combining nuclear and mtDNA data. Both show long-term population expansions since the last glacial episode.

**Fig. 5:** Predicted distributions of *R. parvipalmata* and *R. temporaria* under present, last glacial maximum (LGM; CCSM scenario) and last interglacial (LIG) conditions, based on models built separately for each taxon. Warmer colors indicate higher probabilities of occurrence. All results, including projections combining both taxa in the models, and under the alternative LGM scenario (MIROC), are available in File S8a.

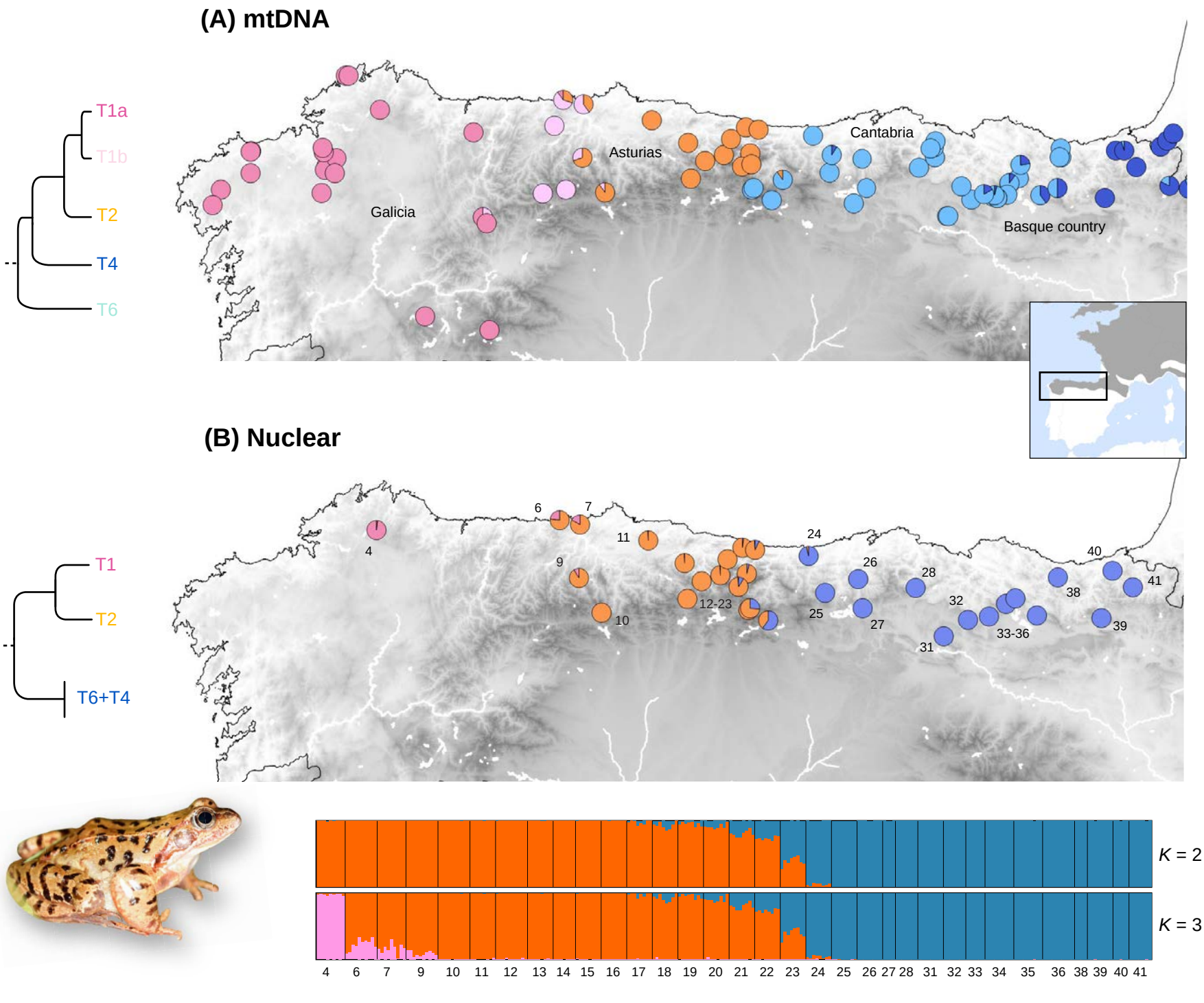
(A) mtDNA
T1a
T1b
T2
T4
T6
Galicia
Asturias
Cantabria
Basque country
(B) Nuclear
T1
T2
T6+T4
4
6
7
9
10
11
12-23
24
25
26
27
28
31
32
33-36
38
39
40
41
K = 2
K = 3
4 6 7 9 10 11 12 13 14 15 16 17 18 19 20 21 22 23 24 25 26 27 28 31 32 33 34 35 36 38 39 40 41

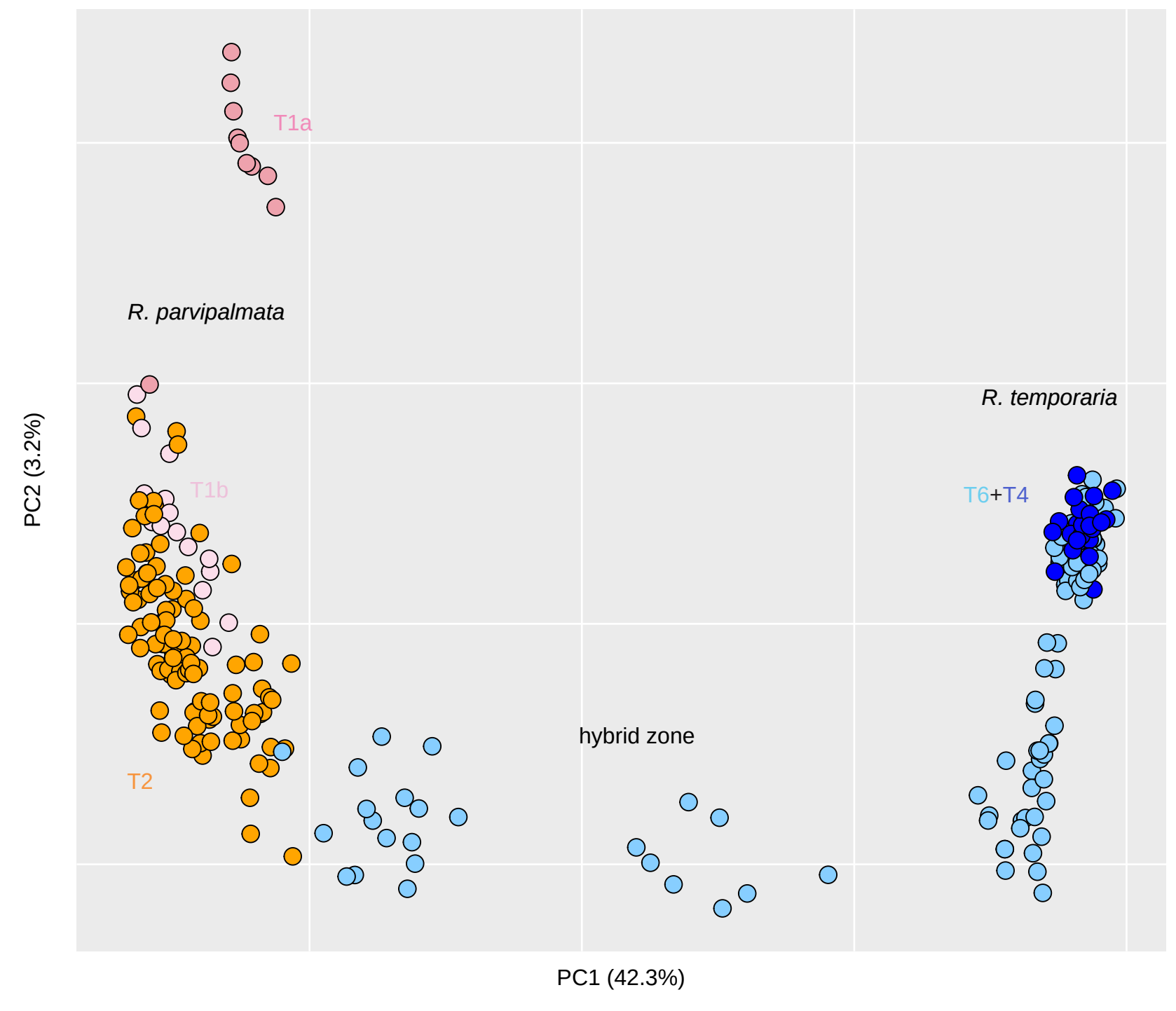
T1a
R. parvipalmata
R. temporaria
T1b
T6+T4
hybrid zone
T2
PC2 (3.2%)
PC1 (42.3%)

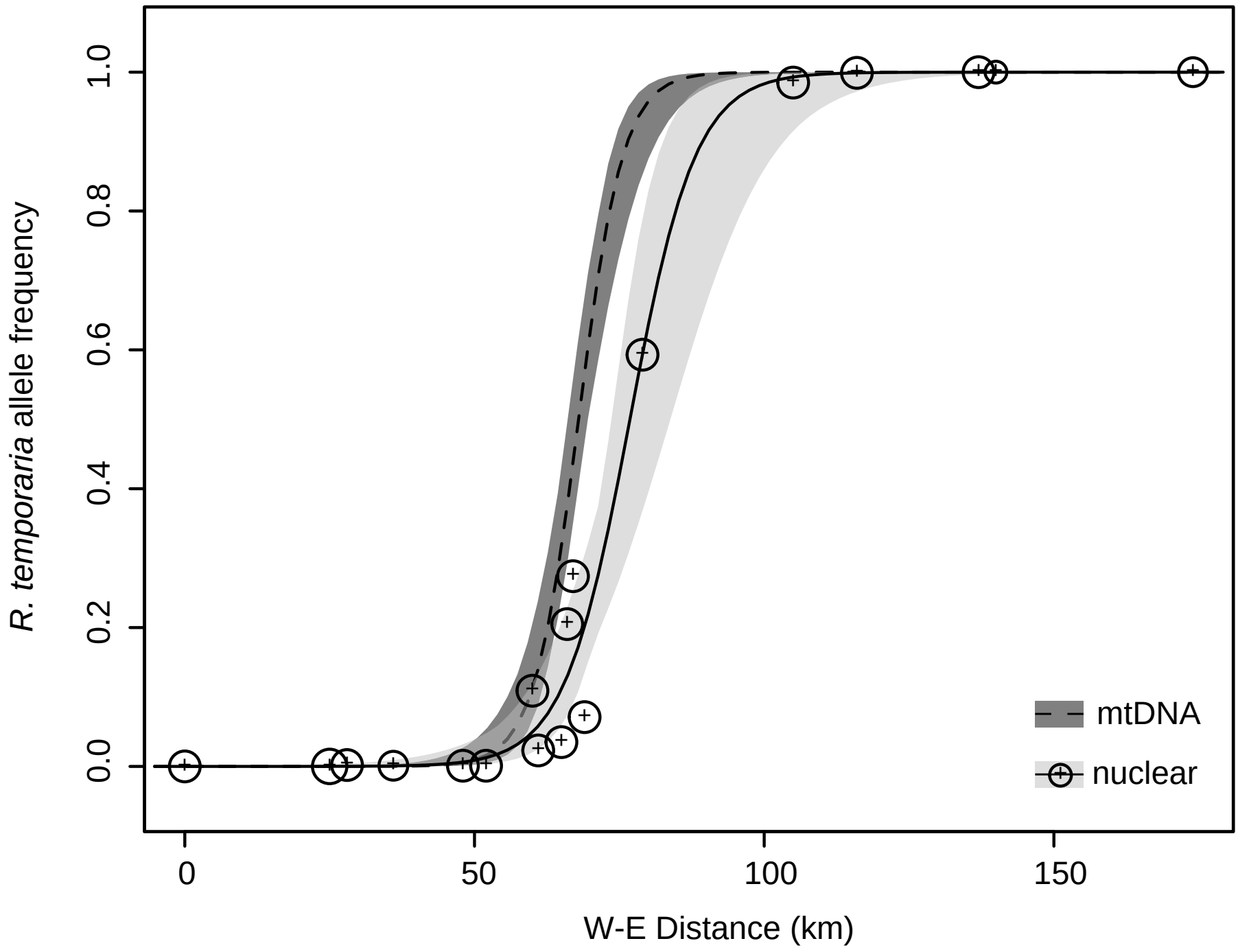
R. temporaria allele frequency
0.0
0.2
0.4
0.6
0.8
1.0
0
50
100
150
W-E Distance (km)
mtDNA
nuclear

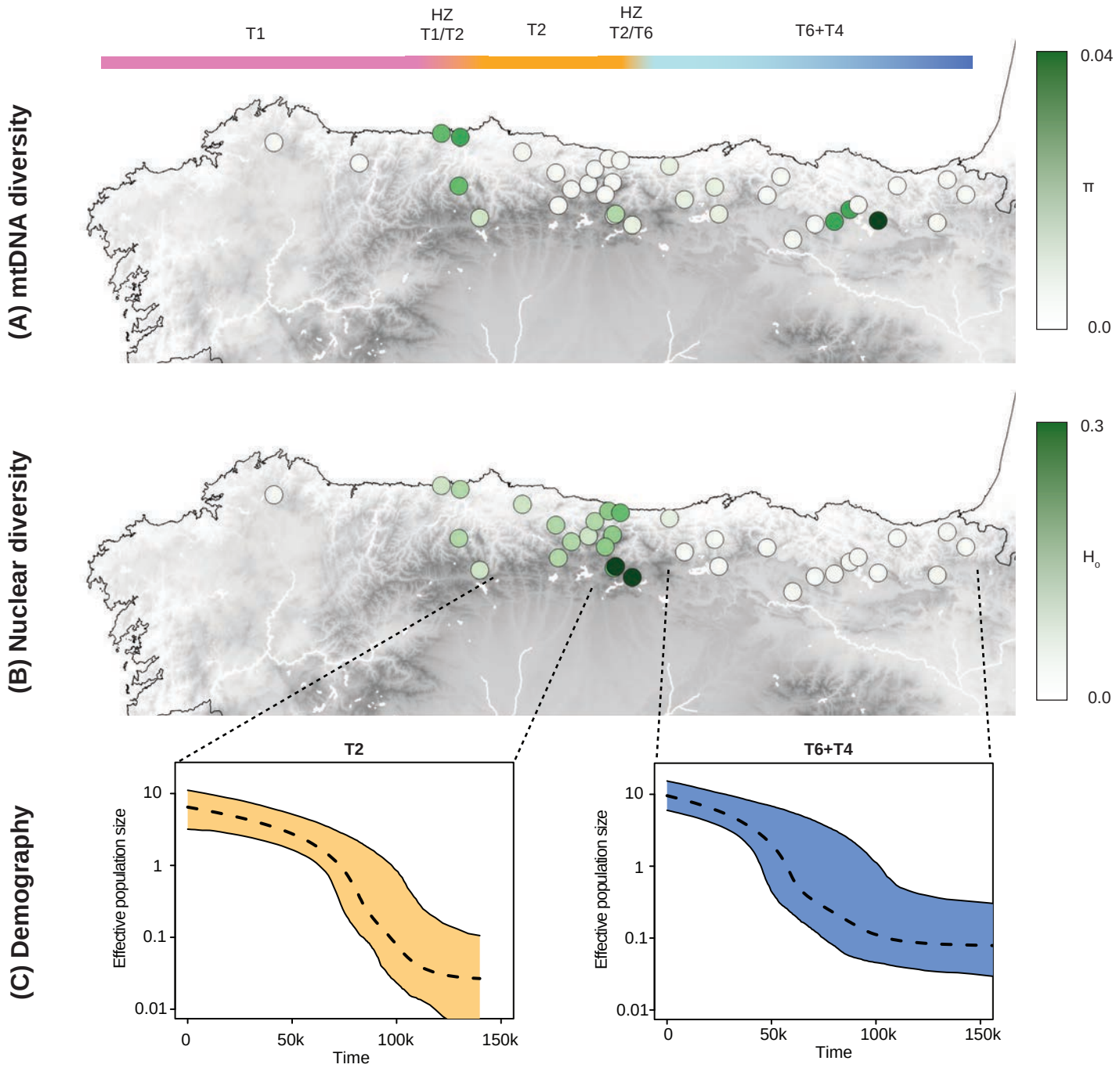
(A) mtDNA diversity
T1
HZ
T1/T2
T2
HZ
T2/T6
T6+T4
0.04
π
0.0
(B) Nuclear diversity
0.3
$H_o$
0.0
(C) Demography
T2
T6+T4
Effective population size
10
1
0.1
0.01
0
50k
100k
150k
Time

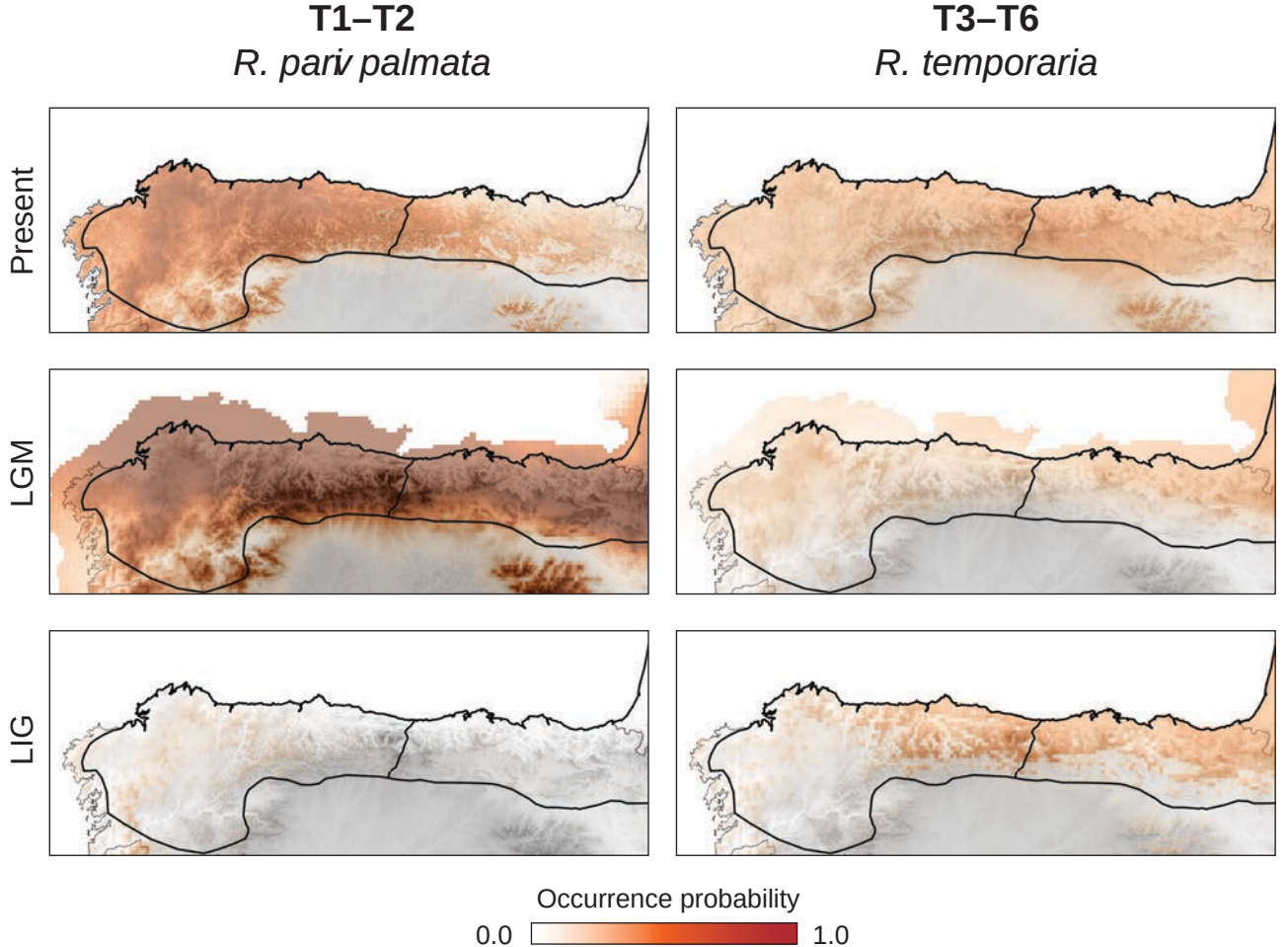
T1–T2
R. pariv palmata
T3–T6
R. temporaria
Present
LGM
LIG
Occurrence probability
0.0
1.0

**File S1:** Details on the individuals of this study, including locality number used on the figures (Loc. ID), individual identifiers (Indiv. ID), geographic information (Lat.: latitude; Long.: longitude), the mtDNA lineage identified by *cyt-b*, and whether samples were included in the nuclear library (RAD) and the nuclear phylogenomics (Phyl.).

| Loc. ID | Indiv. ID | Locality | Lat. | Long. | Sex | mtDNA | RAD | Phyl. |
|---|---|---|---|---|---|---|---|---|
| 1 | IMS3513 | Braña de Cances-Buño | 43.25 | -8.73 | | T1a | | |
| 1 | IMS3514 | Braña de Cances-Buño | 43.25 | -8.73 | | T1a | | |
| 2 | IMS3500 | Arzua | 42.99 | -8.15 | | T1a | | |
| 2 | IMS3501 | Arzua | 42.99 | -8.15 | | T1a | | |
| 2 | IMS3502 | Arzua | 42.99 | -8.15 | | T1a | | |
| 3 | IMS3512 | Coirós | 43.24 | -8.15 | | T1a | | |
| 4 | Rt.Muras.01 | Muras | 43.49 | -7.72 | M | T1a | | |
| 4 | Rt.Muras.02 | Muras | 43.49 | -7.72 | | T1a | x | x |
| 4 | Rt.Muras.03 | Muras | 43.49 | -7.72 | | T1a | x | |
| 4 | Rt.Muras.04 | Muras | 43.49 | -7.72 | | T1a | x | |
| 4 | Rt.Muras.05 | Muras | 43.49 | -7.72 | | T1a | x | x |
| 4 | Rt.Muras.16 | Muras | 43.49 | -7.72 | | T1a | x | x |
| 4 | Rt.Muras.17 | Muras | 43.49 | -7.72 | | T1a | x | |
| 4 | Rt.Muras.18 | Muras | 43.49 | -7.72 | | T1a | x | |
| 4 | Rt.Muras.19 | Muras | 43.49 | -7.72 | | T1a | x | x |
| 4 | Rt.Muras.20 | Muras | 43.49 | -7.72 | | T1a | x | |
| 5 | Rt.Garg.01 | La Garganta | 43.36 | -6.98 | M | T1a | | |
| 5 | Rt.Garg.02 | La Garganta | 43.36 | -6.98 | M | T1a | | |
| 5 | Rt.Garg.03 | La Garganta | 43.36 | -6.98 | M | T1a | | |
| 5 | Rt.Garg.04 | La Garganta | 43.36 | -6.98 | M | T1a | | |
| 5 | Rt.Garg.05 | La Garganta | 43.36 | -6.98 | M | T1a | | |
| 5 | Rt.Garg.06 | La Garganta | 43.36 | -6.98 | M | T1a | | |
| 5 | Rt.Garg.08 | La Garganta | 43.36 | -6.98 | M | T1a | | |
| 5 | Rt.Garg.09 | La Garganta | 43.36 | -6.98 | M | T1a | | |
| 5 | Rt.Garg.10 | La Garganta | 43.36 | -6.98 | M | T1a | | |

| | | | | | | | |
|---|---|---|---|---|---|---|---|
| 6 | Rt.Nove.01 | Novellana | 43.55 | -6.28 | | T1b | x |
| 6 | Rt.Nove.02 | Novellana | 43.55 | -6.28 | | T1b | x |
| 6 | Rt.Nove.03 | Novellana | 43.55 | -6.28 | | T1b | x |
| 6 | Rt.Nove.04 | Novellana | 43.55 | -6.28 | | T1b | x |
| 6 | Rt.Nove.05 | Novellana | 43.55 | -6.28 | | T2 | x |
| 6 | Rt.Nove.06 | Novellana | 43.55 | -6.28 | | T1b | x |
| 6 | Rt.Nove.07 | Novellana | 43.55 | -6.28 | | T2 | x |
| 6 | Rt.Nove.08 | Novellana | 43.55 | -6.28 | | T2 | x |
| 6 | Rt.Nove.09 | Novellana | 43.55 | -6.28 | | T1a | x |
| 6 | Rt.Nove.10 | Novellana | 43.55 | -6.28 | | T1b | x |
| 7 | Rt.Somao.01 | Somao | 43.53 | -6.11 | | T2 | x |
| 7 | Rt.Somao.02 | Somao | 43.53 | -6.11 | | T1b | x |
| 7 | Rt.Somao.03 | Somao | 43.53 | -6.11 | | T1b | x |
| 7 | Rt.Somao.04 | Somao | 43.53 | -6.11 | | T1b | x |
| 7 | Rt.Somao.05 | Somao | 43.53 | -6.11 | | T2 | x |
| 7 | Rt.Somao.06 | Somao | 43.53 | -6.11 | | T2 | x |
| 7 | Rt.Somao.07 | Somao | 43.53 | -6.11 | | T2 | x |
| 7 | Rt.Somao.08 | Somao | 43.53 | -6.11 | | T1b | x |
| 7 | Rt.Somao.09 | Somao | 43.53 | -6.11 | | T1b | x |
| 7 | Rt.Somao.10 | Somao | 43.53 | -6.11 | | T1b | |
| 8 | IMS3560 | Leitariegos | 42.99 | -6.41 | | T1b | |
| 9 | Rt.Marabio.01 | Marabio | 43.21 | -6.11 | M | T2 | x |
| 9 | Rt.Marabio.02 | Marabio | 43.21 | -6.11 | M | T1b | x |
| 9 | Rt.Marabio.03 | Marabio | 43.21 | -6.11 | M | T2 | x |
| 9 | Rt.Marabio.04 | Marabio | 43.21 | -6.11 | M | T1b | x |
| 9 | Rt.Marabio.05 | Marabio | 43.21 | -6.11 | M | T2 | x |
| 9 | Rt.Marabio.06 | Marabio | 43.21 | -6.11 | M | T2 | x |
| 9 | Rt.Marabio.07 | Marabio | 43.21 | -6.11 | M | T2 | x |
| 9 | Rt.Marabio.08 | Marabio | 43.21 | -6.11 | M | T2 | x |
| 9 | Rt.Marabio.09 | Marabio | 43.21 | -6.11 | M | T2 | x |
| 9 | Rt.Marabio.10 | Marabio | 43.21 | -6.11 | M | T1b | x |
| 10 | Rt.Cand.01 | Candioches | 43.00 | -5.92 | | T2 | x |

| | | | | | | | | |
|---|---|---|---|---|---|---|---|---|
| 10 | Rt.Cand.02 | Candioches | 43.00 | -5.92 | | T2 | x | |
| 10 | Rt.Cand.03 | Candioches | 43.00 | -5.92 | | T2 | x | |
| 10 | Rt.Cand.04 | Candioches | 43.00 | -5.92 | | T2 | x | |
| 10 | Rt.Cand.05 | Candioches | 43.00 | -5.92 | | T2 | x | |
| 10 | Rt.Cand.06 | Candioches | 43.00 | -5.92 | | T2 | x | |
| 10 | Rt.Cand.07 | Candioches | 43.00 | -5.92 | | T2 | x | |
| 10 | Rt.Cand.08 | Candioches | 43.00 | -5.92 | | T1b | x | |
| 10 | Rt.Cand.09 | Candioches | 43.00 | -5.92 | | T2 | x | |
| 10 | Rt.Cand.10 | Candioches | 43.00 | -5.92 | | T2 | x | |
| 11 | Rt.Fario.01 | Fario/Fumarea | 43.43 | -5.57 | | T2 | | |
| 11 | Rt.Fario.02 | Fario/Fumarea | 43.43 | -5.57 | | T2 | | |
| 11 | Rt.Fario.03 | Fario/Fumarea | 43.43 | -5.57 | | T2 | x | |
| 11 | Rt.Fumarea.01 | Fario/Fumarea | 43.43 | -5.57 | | T2 | x | x |
| 11 | Rt.Fumarea.02 | Fario/Fumarea | 43.43 | -5.57 | | T2 | x | x |
| 11 | Rt.Fumarea.03 | Fario/Fumarea | 43.43 | -5.57 | | T2 | x | |
| 11 | Rt.Fumarea.04 | Fario/Fumarea | 43.43 | -5.57 | | T2 | x | |
| 11 | Rt.Fumarea.06 | Fario/Fumarea | 43.43 | -5.57 | | T2 | x | |
| 11 | Rt.Fumarea.07 | Fario/Fumarea | 43.43 | -5.57 | | T2 | x | |
| 11 | Rt.Fumarea.08 | Fario/Fumarea | 43.43 | -5.57 | | T2 | x | |
| 11 | Rt.Fumarea.09 | Fario/Fumarea | 43.43 | -5.57 | | T2 | | |
| 11 | Rt.Fumarea.10 | Fario/Fumarea | 43.43 | -5.57 | | T2 | | |
| 12 | Rt.Color.F08 | Color | 43.29 | -5.28 | F | T2 | x | |
| 12 | Rt.Color.F09 | Color | 43.29 | -5.28 | F | T2 | x | x |
| 12 | Rt.Color.F10 | Color | 43.29 | -5.28 | F | T2 | x | x |
| 12 | Rt.Color.F11 | Color | 43.29 | -5.28 | F | T2 | x | |
| 12 | Rt.Color.F12 | Color | 43.29 | -5.28 | F | T2 | x | |
| 12 | Rt.Color.M01 | Color | 43.29 | -5.28 | M | T2 | x | |
| 12 | Rt.Color.M02 | Color | 43.29 | -5.28 | M | T2 | x | |
| 12 | Rt.Color.M03 | Color | 43.29 | -5.28 | M | T2 | x | |
| 12 | Rt.Color.M04 | Color | 43.29 | -5.28 | M | T2 | x | |
| 12 | Rt.Color.M05 | Color | 43.29 | -5.28 | M | T2 | x | |
| 13 | Rt.Senales.01 | Senales | 43.08 | -5.25 | | T2 | x | x |

| | | | | | | | | |
|---|---|---|---|---|---|---|---|---|
| 13 | Rt.Senales.02 | Senales | 43.08 | -5.25 | | T2 | x | x |
| 13 | Rt.Senales.03 | Senales | 43.08 | -5.25 | | T2 | x | |
| 13 | Rt.Senales.04 | Senales | 43.08 | -5.25 | | T2 | x | |
| 13 | Rt.Senales.05 | Senales | 43.08 | -5.25 | | T2 | x | |
| 13 | Rt.Senales.06 | Senales | 43.08 | -5.25 | | T2 | x | |
| 13 | Rt.Senales.07 | Senales | 43.08 | -5.25 | | T2 | x | |
| 13 | Rt.Senales.08 | Senales | 43.08 | -5.25 | | T2 | x | |
| 13 | Rt.Senales.09 | Senales | 43.08 | -5.25 | | T2 | | |
| 13 | Rt.Senales.10 | Senales | 43.08 | -5.25 | | T2 | | |
| 14 | Rt.Bedules.01 | Bedules | 43.19 | -5.14 | | T2 | x | x |
| 14 | Rt.Bedules.02 | Bedules | 43.19 | -5.14 | | T2 | x | |
| 14 | Rt.Bedules.03 | Bedules | 43.19 | -5.14 | | T2 | x | x |
| 14 | Rt.Bedules.04 | Bedules | 43.19 | -5.14 | | T2 | x | |
| 14 | Rt.Bedules.05 | Bedules | 43.19 | -5.14 | | T2 | x | |
| 14 | Rt.Bedules.06 | Bedules | 43.19 | -5.14 | | T2 | x | |
| 14 | Rt.Bedules.07 | Bedules | 43.19 | -5.14 | | T2 | x | |
| 14 | Rt.Bedules.08 | Bedules | 43.19 | -5.14 | | T2 | | |
| 14 | Rt.Bedules.09 | Bedules | 43.19 | -5.14 | | T2 | | |
| 14 | Rt.Bedules.10 | Bedules | 43.19 | -5.14 | | T2 | | |
| 15 | Rt.Llagusecu.F01 | Llagusecu | 43.22 | -4.99 | F | T2 | x | |
| 15 | Rt.Llagusecu.F02 | Llagusecu | 43.22 | -4.99 | F | T2 | x | |
| 15 | Rt.Llagusecu.F03 | Llagusecu | 43.22 | -4.99 | F | T2 | x | |
| 15 | Rt.Llagusecu.F05 | Llagusecu | 43.22 | -4.99 | F | T2 | x | |
| 15 | Rt.Llagusecu.M01 | Llagusecu | 43.22 | -4.99 | M | T2 | x | |
| 15 | Rt.Llagusecu.M02 | Llagusecu | 43.22 | -4.99 | M | T2 | x | |
| 15 | Rt.Llagusecu.M03 | Llagusecu | 43.22 | -4.99 | M | T2 | x | x |
| 15 | Rt.Llagusecu.M04 | Llagusecu | 43.22 | -4.99 | M | T2 | x | x |
| 15 | Rt.Llagusecu.M05 | Llagusecu | 43.22 | -4.99 | M | T2 | | |
| 16 | Rt.Munegru.01 | Cortegueros/Munegru | 43.32 | -4.94 | M | T2 | x | x |
| 16 | Rt.Munegru.02 | Cortegueros/Munegru | 43.32 | -4.94 | M | T2 | x | x |
| 16 | Rt.Munegru.03 | Cortegueros/Munegru | 43.32 | -4.94 | M | T2 | x | |
| 16 | Rt.Munegru.04 | Cortegueros/Munegru | 43.32 | -4.94 | M | T2 | x | |

| | | | | | | | |
|---|---|---|---|---|---|---|---|
| 16 | Rt.Munegru.05 | Cortegueros/Munegru | 43.32 | -4.94 | M | T2 | |
| 16 | Rt.Munegru.33 | Cortegueros/Munegru | 43.32 | -4.94 | F | T2 | x |
| 16 | Rt.Munegru.34 | Cortegueros/Munegru | 43.32 | -4.94 | F | T2 | x |
| 16 | Rt.Munegru.35 | Cortegueros/Munegru | 43.32 | -4.94 | F | T2 | x |
| 16 | Rt.Munegru.36 | Cortegueros/Munegru | 43.32 | -4.94 | F | T2 | x |
| 16 | Rt.Munegru.37 | Cortegueros/Munegru | 43.32 | -4.94 | F | T2 | |
| 17 | Rt.Torneria.01 | Torneria | 43.39 | -4.82 | | T2 | x |
| 17 | Rt.Torneria.02 | Torneria | 43.39 | -4.82 | | T2 | x |
| 17 | Rt.Torneria.03 | Torneria | 43.39 | -4.82 | | T2 | x |
| 17 | Rt.Torneria.04 | Torneria | 43.39 | -4.82 | | T2 | x |
| 17 | Rt.Torneria.11 | Torneria | 43.39 | -4.82 | M | T2 | x |
| 17 | Rt.Torneria.12 | Torneria | 43.39 | -4.82 | M | T2 | x |
| 17 | Rt.Torneria.13 | Torneria | 43.39 | -4.82 | M | T2 | x |
| 17 | Rt.Torneria.14 | Torneria | 43.39 | -4.82 | M | T2 | x |
| 17 | Rt.Torneria.15 | Torneria | 43.39 | -4.82 | M | T2 | |
| 17 | Rt.Torneria.16 | Torneria | 43.39 | -4.82 | M | T2 | |
| 18 | Rt.Puron.01 | Puron | 43.38 | -4.72 | | T2 | x |
| 18 | Rt.Puron.02 | Puron | 43.38 | -4.72 | | T2 | x |
| 18 | Rt.Puron.03 | Puron | 43.38 | -4.72 | | T2 | x |
| 18 | Rt.Puron.04 | Puron | 43.38 | -4.72 | | T2 | x |
| 18 | Rt.Puron.05 | Puron | 43.38 | -4.72 | | T2 | x |
| 18 | Rt.Puron.06 | Puron | 43.38 | -4.72 | | T2 | x |
| 18 | Rt.Puron.07 | Puron | 43.38 | -4.72 | | T2 | x |
| 18 | Rt.Puron.08 | Puron | 43.38 | -4.72 | | T2 | x |
| 18 | Rt.Puron.09 | Puron | 43.38 | -4.72 | | T2 | |
| 18 | Rt.Puron.10 | Puron | 43.38 | -4.72 | | T2 | |
| 19 | Rt.Pande.01 | Pandébano | 43.23 | -4.78 | | T2 | x |
| 19 | Rt.Pande.02 | Pandébano | 43.23 | -4.78 | | T2 | x |
| 19 | Rt.Pande.03 | Pandébano | 43.23 | -4.78 | | T2 | x |
| 19 | Rt.Pande.04 | Pandébano | 43.23 | -4.78 | | T2 | x |
| 19 | Rt.Pande.05 | Pandébano | 43.23 | -4.78 | | T2 | x |
| 19 | Rt.Pande.06 | Pandébano | 43.23 | -4.78 | | T2 | x |

| | | | | | | | |
|---|---|---|---|---|---|---|---|
| 19 | Rt.Pande.07 | Pandébano | 43.23 | -4.78 | | T2 | x |
| 19 | Rt.Pande.09 | Pandébano | 43.23 | -4.78 | | T2 | x |
| 19 | Rt.Pande.10 | Pandébano | 43.23 | -4.78 | | T2 | |
| 20 | Rt.Liordes.01 | Liordes | 43.15 | -4.84 | | T2 | x |
| 20 | Rt.Liordes.02 | Liordes | 43.15 | -4.84 | | T2 | x |
| 20 | Rt.Liordes.03 | Liordes | 43.15 | -4.84 | | T2 | x |
| 20 | Rt.Liordes.04 | Liordes | 43.15 | -4.84 | | T2 | x |
| 20 | Rt.Liordes.05 | Liordes | 43.15 | -4.84 | | T2 | x |
| 20 | Rt.Liordes.06 | Liordes | 43.15 | -4.84 | | T2 | x |
| 20 | Rt.Liordes.08 | Liordes | 43.15 | -4.84 | | T2 | x |
| 20 | Rt.Liordes.09 | Liordes | 43.15 | -4.84 | | T2 | x |
| 20 | Rt.Liordes.10 | Liordes | 43.15 | -4.84 | | T2 | |
| 21 | Rt.HVargas.01 | Hoyos De Vargas | 43.01 | -4.76 | M | T6 | x |
| 21 | Rt.HVargas.02 | Hoyos De Vargas | 43.01 | -4.76 | | T6 | x |
| 21 | Rt.HVargas.03 | Hoyos De Vargas | 43.01 | -4.76 | | T6 | x |
| 21 | Rt.HVargas.04 | Hoyos De Vargas | 43.01 | -4.76 | | T6 | x |
| 21 | Rt.HVargas.05 | Hoyos De Vargas | 43.01 | -4.76 | | T6 | x |
| 21 | Rt.HVargas.06 | Hoyos De Vargas | 43.01 | -4.76 | | T6 | x |
| 21 | Rt.HVargas.07 | Hoyos De Vargas | 43.01 | -4.76 | | T6 | x |
| 21 | Rt.HVargas.08 | Hoyos De Vargas | 43.01 | -4.76 | | T6 | x |
| 21 | Rt.HVargas.09 | Hoyos De Vargas | 43.01 | -4.76 | | T6 | |
| 21 | Rt.HVargas.10 | Hoyos De Vargas | 43.01 | -4.76 | | T6 | |
| 22 | Rt.Hemp.01 | Hoyos Empedrado | 43.02 | -4.75 | M | T6 | x |
| 22 | Rt.Hemp.02 | Hoyos Empedrado | 43.02 | -4.75 | F | T6 | x |
| 22 | Rt.Hemp.03 | Hoyos Empedrado | 43.02 | -4.75 | M | T6 | x |
| 22 | Rt.Hemp.04 | Hoyos Empedrado | 43.02 | -4.75 | F | T6 | x |
| 22 | Rt.Hemp.06 | Hoyos Empedrado | 43.02 | -4.75 | F | T6 | x |
| 22 | Rt.Hemp.08 | Hoyos Empedrado | 43.02 | -4.75 | F | T6 | x |
| 22 | Rt.Hemp.09 | Hoyos Empedrado | 43.02 | -4.75 | M | T6 | x |
| 22 | Rt.Hemp.10 | Hoyos Empedrado | 43.02 | -4.75 | F | T6 | |
| 22 | Rt.Hemp.11 | Hoyos Empedrado | 43.02 | -4.75 | M | T6 | x |
| 22 | Rt.Hemp.12 | Hoyos Empedrado | 43.02 | -4.75 | M | T6 | |

| | | | | | | | |
|---|---|---|---|---|---|---|---|
| 23 | Rt.Vidrieros.01 | Vidrieros | 42.95 | -4.60 | | T6 | x |
| 23 | Rt.Vidrieros.02 | Vidrieros | 42.95 | -4.60 | | T6 | x |
| 23 | Rt.Vidrieros.03 | Vidrieros | 42.95 | -4.60 | | T6 | x |
| 23 | Rt.Vidrieros.04 | Vidrieros | 42.95 | -4.60 | | T6 | x |
| 23 | Rt.Vidrieros.05 | Vidrieros | 42.95 | -4.60 | | T6 | x |
| 23 | Rt.Vidrieros.06 | Vidrieros | 42.95 | -4.60 | | T6 | x |
| 23 | Rt.Vidrieros.07 | Vidrieros | 42.95 | -4.60 | | T6 | x |
| 23 | Rt.Vidrieros.08 | Vidrieros | 42.95 | -4.60 | | T6 | x |
| 23 | Rt.Vidrieros.09 | Vidrieros | 42.95 | -4.60 | | T6 | |
| 23 | Rt.Vidrieros.10 | Vidrieros | 42.95 | -4.60 | | T6 | |
| 24 | Rt.MCorona.01 | Monte Corona | 43.34 | -4.29 | | T6 | x |
| 24 | Rt.MCorona.02 | Monte Corona | 43.34 | -4.29 | | T6 | x |
| 24 | Rt.MCorona.03 | Monte Corona | 43.34 | -4.29 | | T6 | x |
| 24 | Rt.MCorona.04 | Monte Corona | 43.34 | -4.29 | | T6 | x |
| 24 | Rt.MCorona.05 | Monte Corona | 43.34 | -4.29 | | T6 | x |
| 24 | Rt.MCorona.06 | Monte Corona | 43.34 | -4.29 | | T6 | x |
| 24 | Rt.MCorona.07 | Monte Corona | 43.34 | -4.29 | | T6 | x |
| 24 | Rt.MCorona.08 | Monte Corona | 43.34 | -4.29 | | T6 | x |
| 24 | Rt.MCorona.09 | Monte Corona | 43.34 | -4.29 | | T6 | |
| 24 | Rt.MCorona.10 | Monte Corona | 43.34 | -4.29 | | T6 | |
| 25 | Rt.Barcena.01 | Barcena | 43.12 | -4.16 | M | T6 | x |
| 25 | Rt.Barcena.02 | Barcena | 43.12 | -4.16 | M | T6 | x |
| 25 | Rt.Barcena.03 | Barcena | 43.12 | -4.16 | M | T6 | x |
| 25 | Rt.Barcena.04 | Barcena | 43.12 | -4.16 | M | T6 | x |
| 25 | Rt.Barcena.05 | Barcena | 43.12 | -4.16 | M | T6 | x |
| 25 | Rt.Barcena.06 | Barcena | 43.12 | -4.16 | M | T6 | x |
| 25 | Rt.Barcena.07 | Barcena | 43.12 | -4.16 | M | T6 | x |
| 25 | Rt.Barcena.09 | Barcena | 43.12 | -4.16 | M | T6 | |
| 25 | Rt.Barcena.17 | Barcena | 43.12 | -4.16 | F | T6 | x |
| 26 | Rt.Alc.01 | Alceda | 43.20 | -3.90 | M | T6 | x |
| 26 | Rt.Alc.02 | Alceda | 43.20 | -3.90 | | T6 | x |
| 26 | Rt.Alc.03 | Alceda | 43.20 | -3.90 | | T6 | x |

| | | | | | | | | |
|---|---|---|---|---|---|---|---|---|
| 26 | Rt.Alc.04 | Alceda | 43.20 | -3.90 | | T6 | x | |
| 26 | Rt.Alc.05 | Alceda | 43.20 | -3.90 | | T6 | x | |
| 26 | Rt.Alc.06 | Alceda | 43.20 | -3.90 | | T6 | x | |
| 26 | Rt.Alc.07 | Alceda | 43.20 | -3.90 | | T6 | x | x |
| 26 | Rt.Alc.08 | Alceda | 43.20 | -3.90 | | T6 | x | x |
| 26 | Rt.Alc.09 | Alceda | 43.20 | -3.90 | | T6 | | |
| 26 | Rt.Alc.10 | Alceda | 43.20 | -3.90 | | T6 | | |
| 27 | Rt.Ebro.01 | Embalse del Ebro | 43.02 | -3.86 | M | T6 | | |
| 27 | Rt.Ebro.02 | Embalse del Ebro | 43.02 | -3.86 | M | T6 | x | x |
| 27 | Rt.Ebro.03 | Embalse del Ebro | 43.02 | -3.86 | M | T6 | | |
| 27 | Rt.Ebro.04 | Embalse del Ebro | 43.02 | -3.86 | M | T6 | x | x |
| 27 | Rt.Ebro.05 | Embalse del Ebro | 43.02 | -3.86 | M | T6 | x | |
| 27 | Rt.Ebro.06 | Embalse del Ebro | 43.02 | -3.86 | M | T6 | | |
| 27 | Rt.Ebro.07 | Embalse del Ebro | 43.02 | -3.86 | M | T6 | | |
| 27 | Rt.Ebro.08 | Embalse del Ebro | 43.02 | -3.86 | M | T6 | | |
| 27 | Rt.Ebro.13 | Embalse del Ebro | 43.02 | -3.86 | F | T6 | | |
| 27 | Rt.Ebro.15 | Embalse del Ebro | 43.02 | -3.86 | F | T6 | x | |
| 28 | Rt.Aguer.01 | Aguera | 43.15 | -3.45 | | T6 | x | |
| 28 | Rt.Aguer.02 | Aguera | 43.15 | -3.45 | | T6 | | |
| 28 | Rt.Aguer.03 | Aguera | 43.15 | -3.45 | | T6 | x | |
| 28 | Rt.Aguer.04 | Aguera | 43.15 | -3.45 | | T6 | x | |
| 28 | Rt.Aguer.05 | Aguera | 43.15 | -3.45 | | T6 | x | |
| 28 | Rt.Aguer.06 | Aguera | 43.15 | -3.45 | | T6 | x | |
| 28 | Rt.Aguer.07 | Aguera | 43.15 | -3.45 | | T6 | x | x |
| 28 | Rt.Aguer.08 | Aguera | 43.15 | -3.45 | | T6 | x | x |
| 28 | Rt.Aguer.09 | Aguera | 43.15 | -3.45 | | T6 | | |
| 28 | Rt.Aguer.10 | Aguera | 43.15 | -3.45 | | T6 | | |
| 29 | Rt.Pando.01 | Pando | 43.21 | -3.32 | | T6 | | |
| 30 | RTe10 | Sopeña5 | 43.27 | -3.32 | | T6 | | |
| 30 | RTe3 | Sopeña2 | 43.27 | -3.33 | | T6 | | |
| 30 | RTe4 | Sopeña2 | 43.27 | -3.33 | | T6 | | |
| 30 | RTe6 | Sopeña4 | 43.27 | -3.33 | | T6 | | |

| | | | | | | | | |
|---|---|---|---|---|---|---|---|---|
| 30 | RTe7 | Sopeña4 | 43.27 | -3.33 | | T6 | | |
| 30 | RTe8 | Sopeña4 | 43.27 | -3.33 | | T6 | | |
| 30 | RTe9 | Sopeña5 | 43.27 | -3.32 | | T6 | | |
| 31 | PNValderejo-1 | Charca Cruz de San Miguel, PN Valderejo | 42.87 | -3.23 | | T6 | x | x |
| 31 | PNValderejo-2 | Charca Cruz de San Miguel, PN Valderejo | 42.87 | -3.23 | | T6 | x | x |
| 31 | PNValderejo-3 | Rodada de pista, PN Valderejo | 42.86 | -3.20 | | T6 | x | |
| 31 | PNValderejo-4 | Rodada de pista, PN Valderejo | 42.86 | -3.20 | | T6 | x | |
| 31 | PNValderejo-5 | Rodada de pista, PN Valderejo | 42.86 | -3.20 | | T6 | x | |
| 31 | PNValderejo-6 | Charca Solinde II, PN Valderejo | 42.85 | -3.21 | | T6 | x | |
| 31 | PNValderejo-7 | Rodada de pista, PN Valderejo | 42.86 | -3.20 | | T6 | x | |
| 31 | PNValderejo-8 | Charca Cruz de San Miguel, PN Valderejo | 42.87 | -3.23 | | T6 | x | |
| 31 | PNValderejo-9 | Charca Cruz de San Miguel, PN Valderejo | 42.87 | -3.23 | | T6 | | |
| 31 | PNValderejo-10 | Charca Cruz de San Miguel, PN Valderejo | 42.87 | -3.23 | | T6 | | |
| 32 | Rt.Terl.01 | Tertanga | 42.96 | -3.03 | M | T6 | x | |
| 32 | Rt.Terl.02 | Tertanga | 42.96 | -3.03 | M | T6 | x | |
| 32 | Rt.Terl.03 | Tertanga | 42.96 | -3.03 | M | T6 | x | |
| 32 | Rt.Terl.04 | Tertanga | 42.96 | -3.03 | M | T6 | | |
| 32 | Rt.Terl.05 | Tertanga | 42.96 | -3.03 | M | T6 | x | |
| 32 | Rt.Terl.06 | Tertanga | 42.96 | -3.03 | M | T6 | x | |
| 32 | Rt.Terl.07 | Tertanga | 42.96 | -3.03 | M | T6 | x | |
| 32 | Rt.Terl.08 | Tertanga | 42.96 | -3.03 | M | T6 | x | |
| 32 | Rt.Terl.09 | Tertanga | 42.96 | -3.03 | M | T6 | | |
| 32 | Rt.Terl.10 | Tertanga | 42.96 | -3.03 | M | T6 | | |
| 33 | RTe61 | Altube1 | 42.97 | -2.86 | | T6 | x | |
| 33 | RTe62 | Altube1 | 42.97 | -2.86 | | T6 | x | |
| 33 | RTe63 | Altube2 | 42.98 | -2.86 | | T6 | x | |
| 33 | RTe64 | Altube2 | 42.98 | -2.86 | | T6 | x | |
| 33 | RTe65 | Altube2 | 42.98 | -2.86 | | T6 | x | |
| 33 | RTe66 | Altube2 | 42.98 | -2.86 | | T4 | x | |
| 34 | RTe31 | Saldropo | 43.05 | -2.73 | | T6 | x | |
| 34 | RTe32 | Saldropo | 43.05 | -2.73 | | T6 | x | |
| 34 | RTe33 | Saldropo | 43.05 | -2.73 | | T6 | x | |

| | | | | | | | |
|---|---|---|---|---|---|---|---|
| 34 | RTe34 | Saldropo | 43.05 | -2.73 | | T6 | x |
| 34 | RTe35 | Saldropo | 43.05 | -2.73 | | T6 | x |
| 34 | RTe36 | Saldropo | 43.05 | -2.73 | | T6 | x |
| 34 | RTe37 | Saldropo | 43.05 | -2.73 | | T6 | x |
| 34 | RTe38 | Saldropo | 43.05 | -2.73 | | T6 | x |
| 34 | RTe39 | Saldropo | 43.05 | -2.73 | | T4 | x |
| 34 | RTe40 | Saldropo | 43.05 | -2.73 | | T6 | |
| 35 | RTe21 | Urkiola1 | 43.09 | -2.65 | | T6 | x |
| 35 | RTe22 | Urkiola1 | 43.09 | -2.65 | | T6 | x |
| 35 | RTe23 | Urkiola2 | 43.08 | -2.66 | | T6 | x |
| 35 | RTe24 | Urkiola3 | 43.09 | -2.67 | | T6 | x |
| 35 | RTe25 | Urkiola3 | 43.09 | -2.67 | | T6 | x |
| 35 | RTe26 | Urkiola4 | 43.09 | -2.67 | | T6 | x |
| 35 | RTe27 | Urkiola4 | 43.09 | -2.67 | | T6 | x |
| 35 | RTe28 | Urkiola5 | 43.09 | -2.66 | | T6 | x |
| 35 | RTe29 | Urkiola6 | 43.09 | -2.65 | | T6 | x |
| 35 | RTe30 | Urkiola7 | 43.08 | -2.65 | | T6 | |
| 36 | RTe51 | Aizkorri | 42.98 | -2.48 | | T6 | x |
| 36 | RTe52 | Aizkorri | 42.98 | -2.48 | | T4 | x |
| 36 | RTe53 | Aizkorri | 42.98 | -2.48 | | T6 | x |
| 36 | RTe54 | Aizkorri | 42.98 | -2.48 | | T6 | x |
| 36 | RTe55 | Aizkorri | 42.98 | -2.48 | | T6 | x |
| 36 | RTe56 | Aizkorri | 42.98 | -2.48 | | T4 | x |
| 36 | RTe57 | Aizkorri | 42.98 | -2.48 | | T4 | x |
| 36 | RTe58 | Aizkorri | 42.98 | -2.48 | | T6 | x |
| 36 | RTe59 | Aizkorri | 42.98 | -2.48 | | T6 | x |
| 36 | RTe60 | Aizkorri | 42.98 | -2.48 | | T4 | x |
| 37 | Rt.Itz.01 | Itziar | 43.26 | -2.33 | F | T6 | |
| 38 | Rt.Bust.01 | Elgoibar | 43.21 | -2.32 | F | T6 | x |
| 38 | Rt.Bust.02 | Elgoibar | 43.21 | -2.32 | F | T6 | x |
| 38 | Rt.Bust.03 | Elgoibar | 43.21 | -2.32 | M | T6 | |
| 38 | Rt.Bust.04 | Elgoibar | 43.21 | -2.32 | M | T6 | x |

| | | | | | | | | |
|---|---|---|---|---|---|---|---|---|
| 38 | Rt.Bust.05 | Elgoibar | 43.21 | -2.32 | F | T6 | x | |
| 39 | RTe41 | Aralar | 42.97 | -1.97 | | T4 | x | |
| 39 | RTe42 | Aralar | 42.97 | -1.97 | | T4 | x | |
| 39 | RTe43 | Aralar | 42.97 | -1.97 | | T4 | x | |
| 39 | RTe44 | Aralar | 42.97 | -1.97 | | T4 | x | |
| 39 | RTe45 | Aralar | 42.97 | -1.97 | | T4 | x | |
| 39 | RTe46 | Aralar | 42.97 | -1.97 | | T4 | x | |
| 39 | RTe47 | Aralar | 42.97 | -1.97 | | T4 | x | x |
| 39 | RTe48 | Aralar | 42.97 | -1.97 | | T4 | x | x |
| 39 | RTe49 | Aralar | 42.96 | -1.98 | | T4 | | |
| 39 | RTe50 | Aralar | 42.96 | -1.98 | | T4 | | |
| 40 | AIA-01-M | Aiako Harria (charca de Malbazar) | 43.25 | -1.89 | M | T4 | x | x |
| 40 | AIA-02-M | Aiako Harria (charca de Malbazar) | 43.25 | -1.89 | M | T4 | x | x |
| 40 | AIA-03-M | Aiako Harria (charca de Malbazar) | 43.25 | -1.89 | M | T4 | x | |
| 40 | AIA-04-M | Aiako Harria (charca de Malbazar) | 43.25 | -1.89 | M | T4 | x | |
| 40 | AIA-05-M | Aiako Harria (charca de Malbazar) | 43.25 | -1.89 | M | T4 | | |
| 40 | AIA-06-M | Aiako Harria (charca de Malbazar) | 43.25 | -1.89 | M | T4 | | |
| 40 | AIA-11-F | Aiako Harria (charca de Malbazar) | 43.25 | -1.89 | F | T4 | x | |
| 41 | Rt.Aur.01 | Aurtitz | 43.15 | -1.73 | M | T4 | x | x |
| 41 | Rt.Aur.02 | Aurtitz | 43.15 | -1.73 | F | T4 | x | x |
| 41 | Rt.Aur.03 | Aurtitz | 43.15 | -1.73 | F | T4 | x | |
| 41 | Rt.Aur.04 | Aurtitz | 43.15 | -1.73 | F | T4 | | |
| 41 | Rt.Aur.05 | Aurtitz | 43.15 | -1.73 | F | T4 | x | |
| 41 | Rt.Aur.06 | Aurtitz | 43.15 | -1.73 | M | T4 | x | |
| 41 | Rt.Aur.07 | Aurtitz | 43.15 | -1.73 | M | T4 | x | |
| 41 | Rt.Aur.08 | Aurtitz | 43.15 | -1.73 | M | T4 | x | |
| 41 | Rt.Aur.09 | Aurtitz | 43.15 | -1.73 | M | T4 | | |

MOLECULAR ECOLOGY

Supplementary Material for:

# Are glacial refugia hotspots of cryptic speciation and of cyto-nuclear discordances? Answers from the genomic phylogeography of Spanish common frogs

Christophe Dufresnes, Alfredo G. Nicieza, Spartak N. Litvinchuk, Nicolas Rodrigues, Daniel L. Jeffries, Miguel Vences, Nicolas Perrin, and Íñigo Martínez-Solano

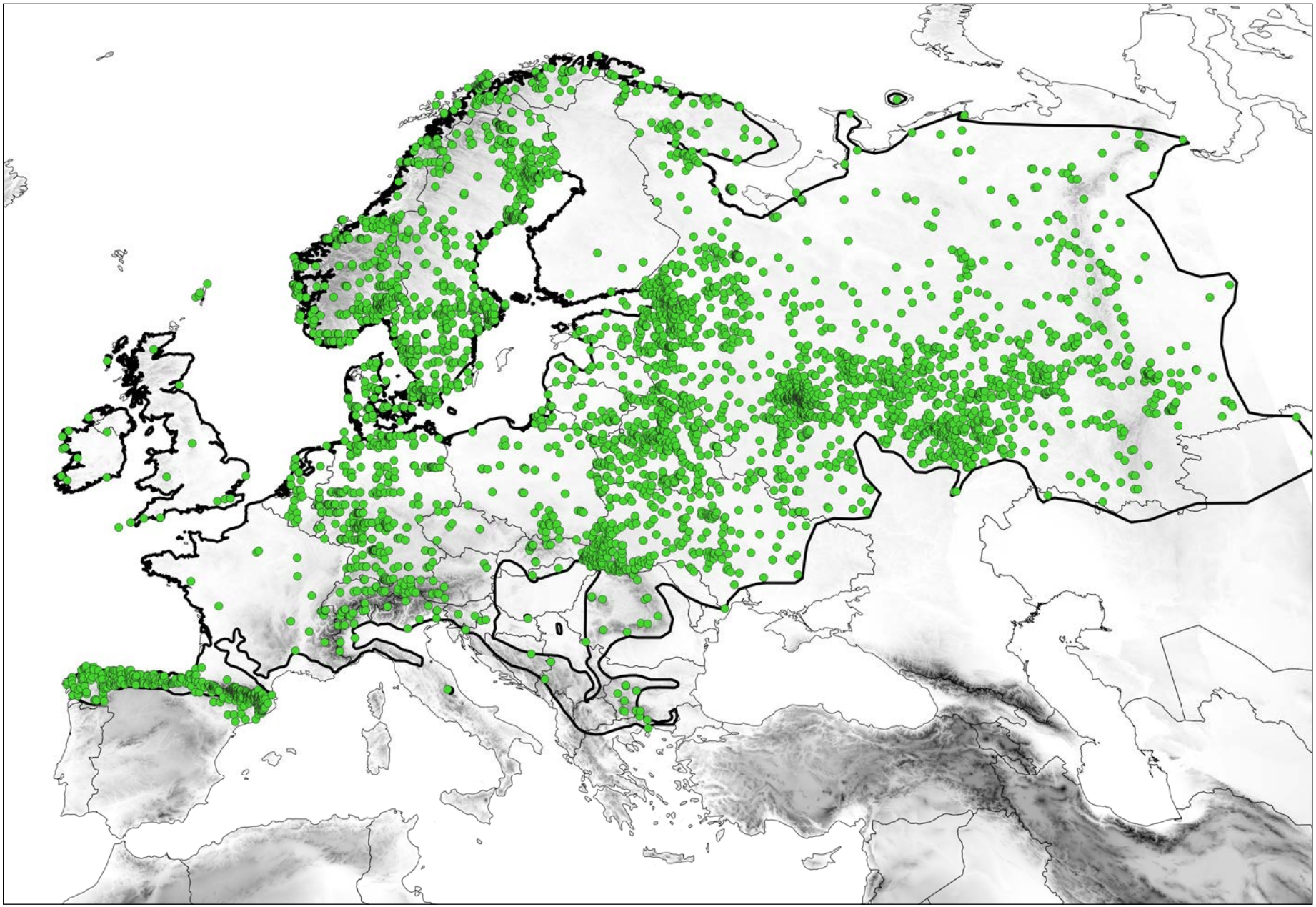

**File S2:** Occurrence data used in the niche modelling analyses. The thick black line shows the known distributions of the species.

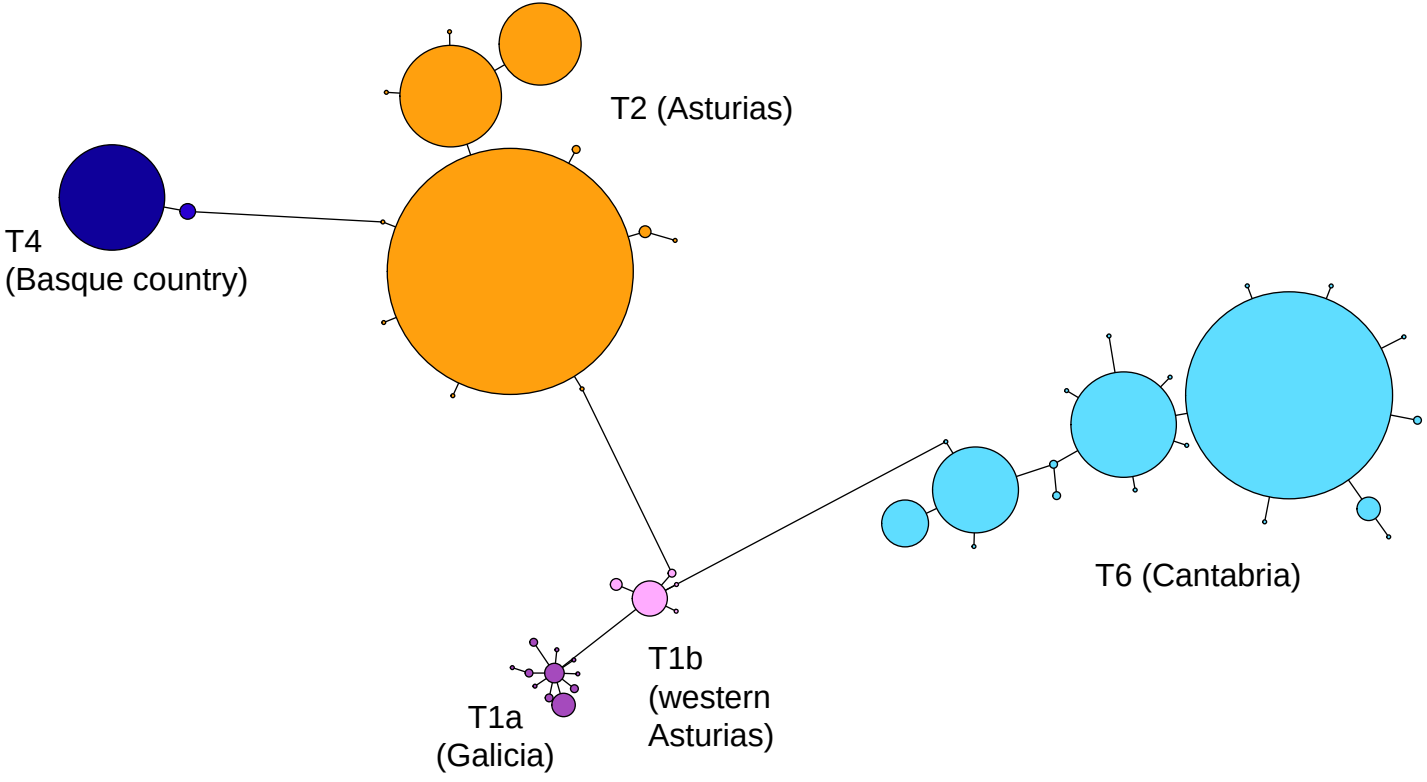


**File S3a**: Network of 50 mitochondrial *cyt-b* haplotypes (501bp) sequenced in 331 samples from Northern Spain.

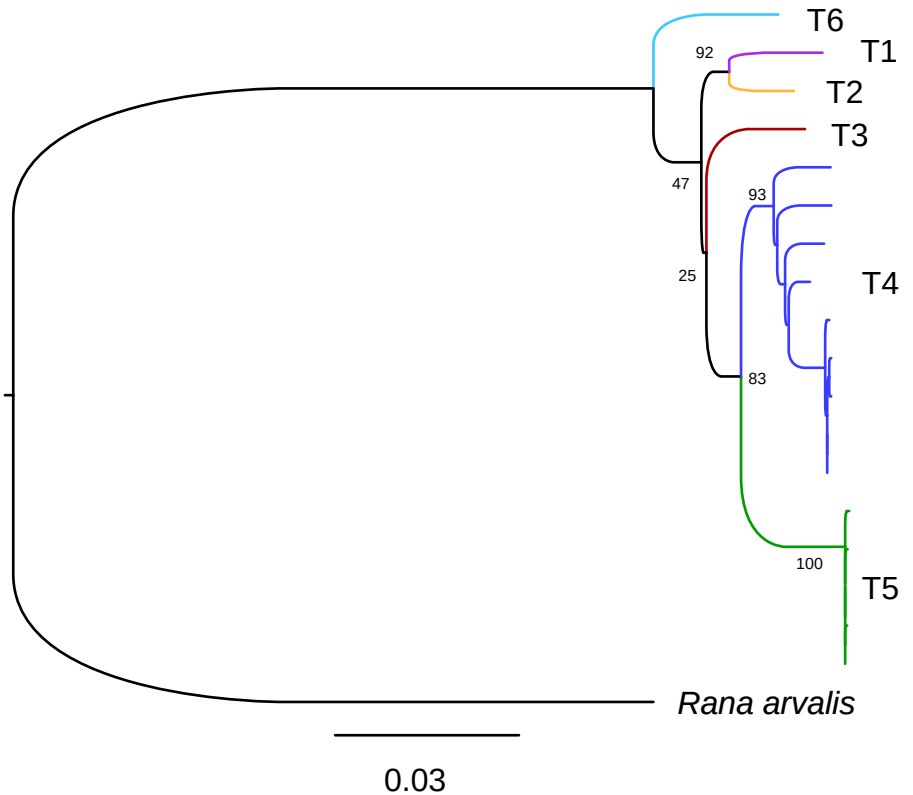


**File S3b:** Maximum-likelihood mitochondrial phylogeny of common frogs, with *Rana arvalis* as outgroup, based on six genes and stretches of tRNA (data from Vences et al. 2017), totalling 4,278 bp.

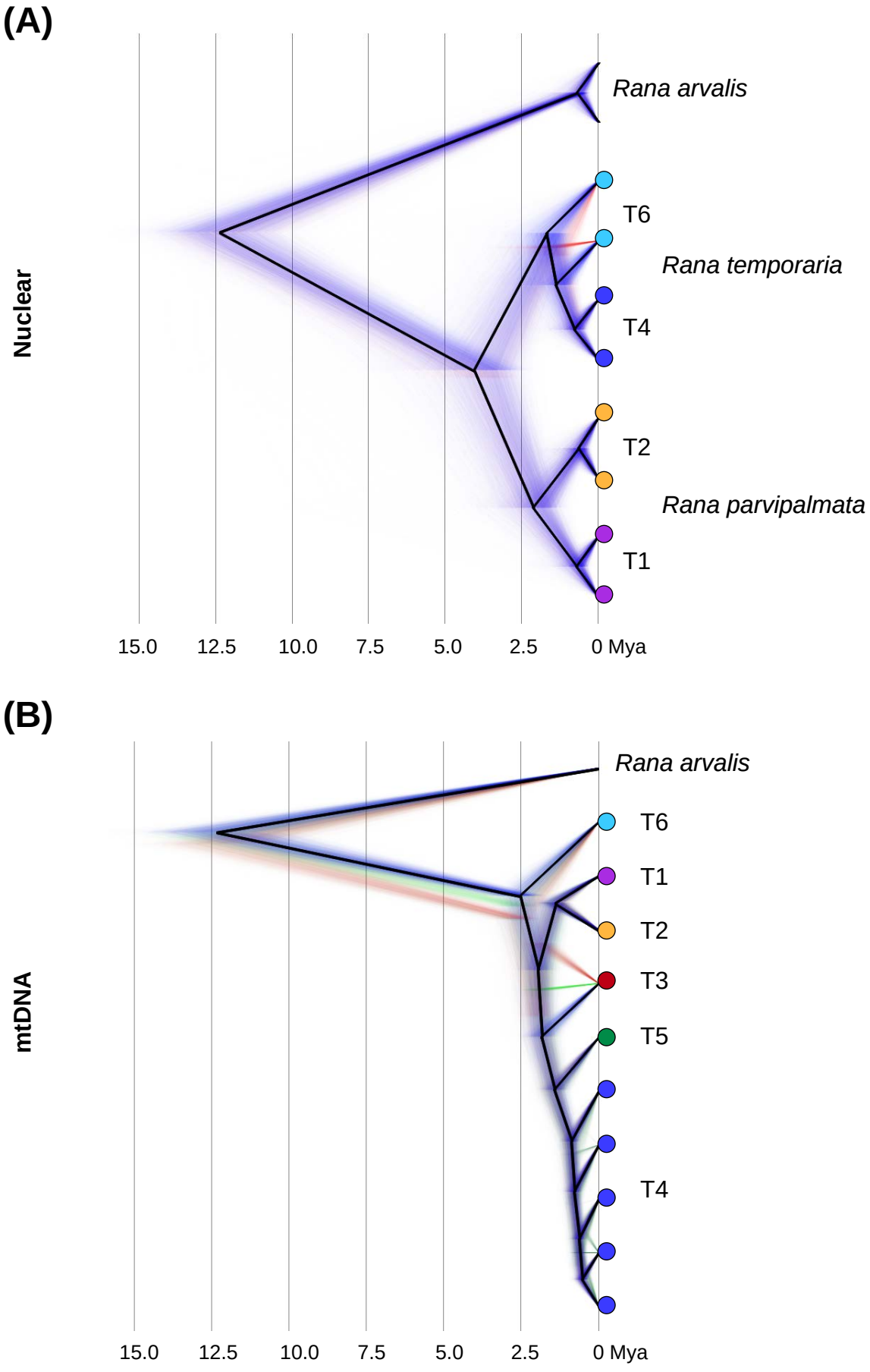


**File S3c:** Time-calibrated phylogenies on subsets of (A) nuclear concatenated sequences (142kb from 1,207 RAD tags) and (B) on mitochondrial haplotypes (4.3kb from six genes and stretches of tRNA).

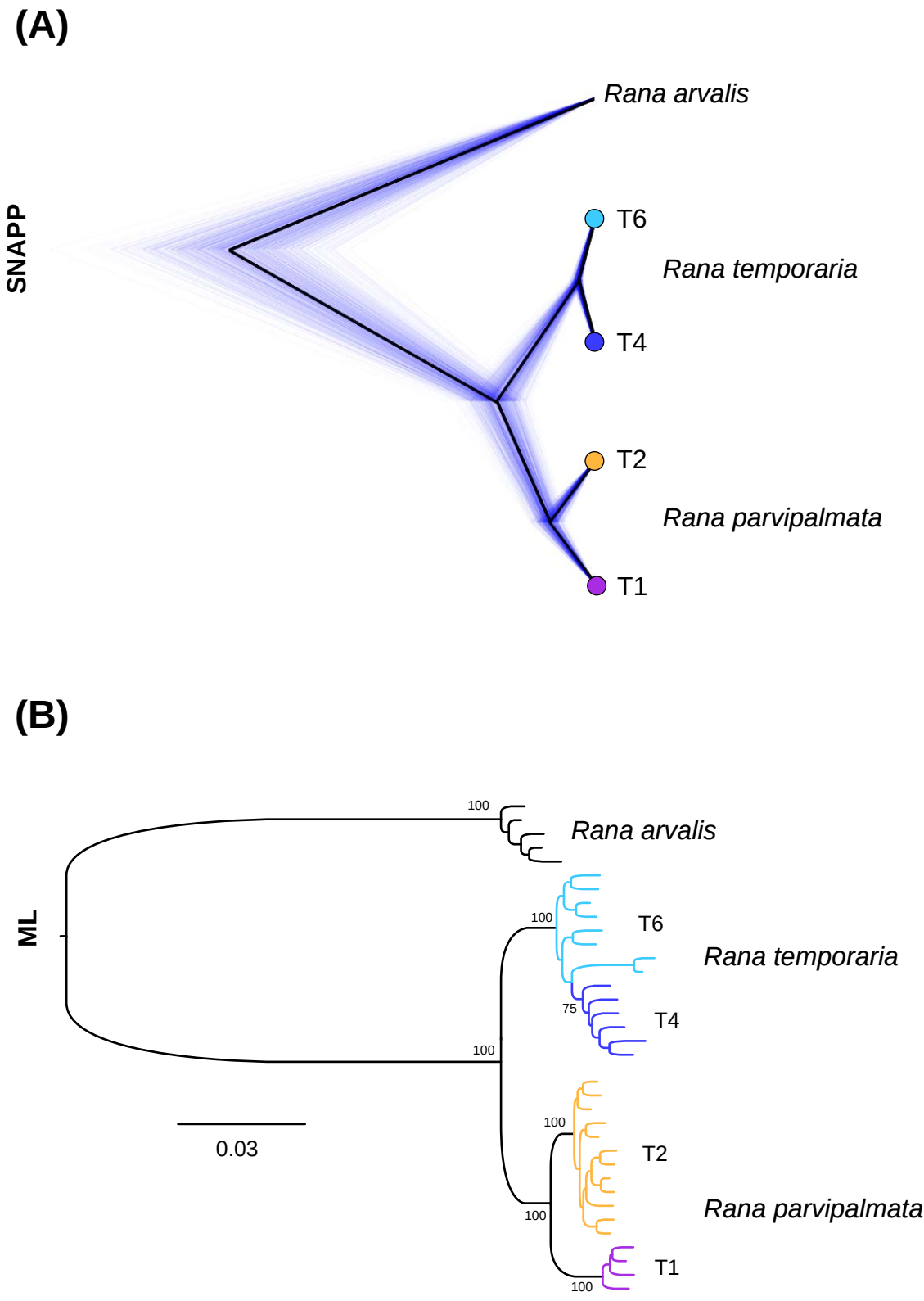


**File S3d:** Nuclear phylogenies of northern spanish common frogs, with *Rana arvalis* as outgroup, using (A) SNAPP on SNP data (cloudogram of the species trees) and (B) PhyML on concatenated sequence data (cladogram of the samples: bootstrap support is indicated for major nodes).

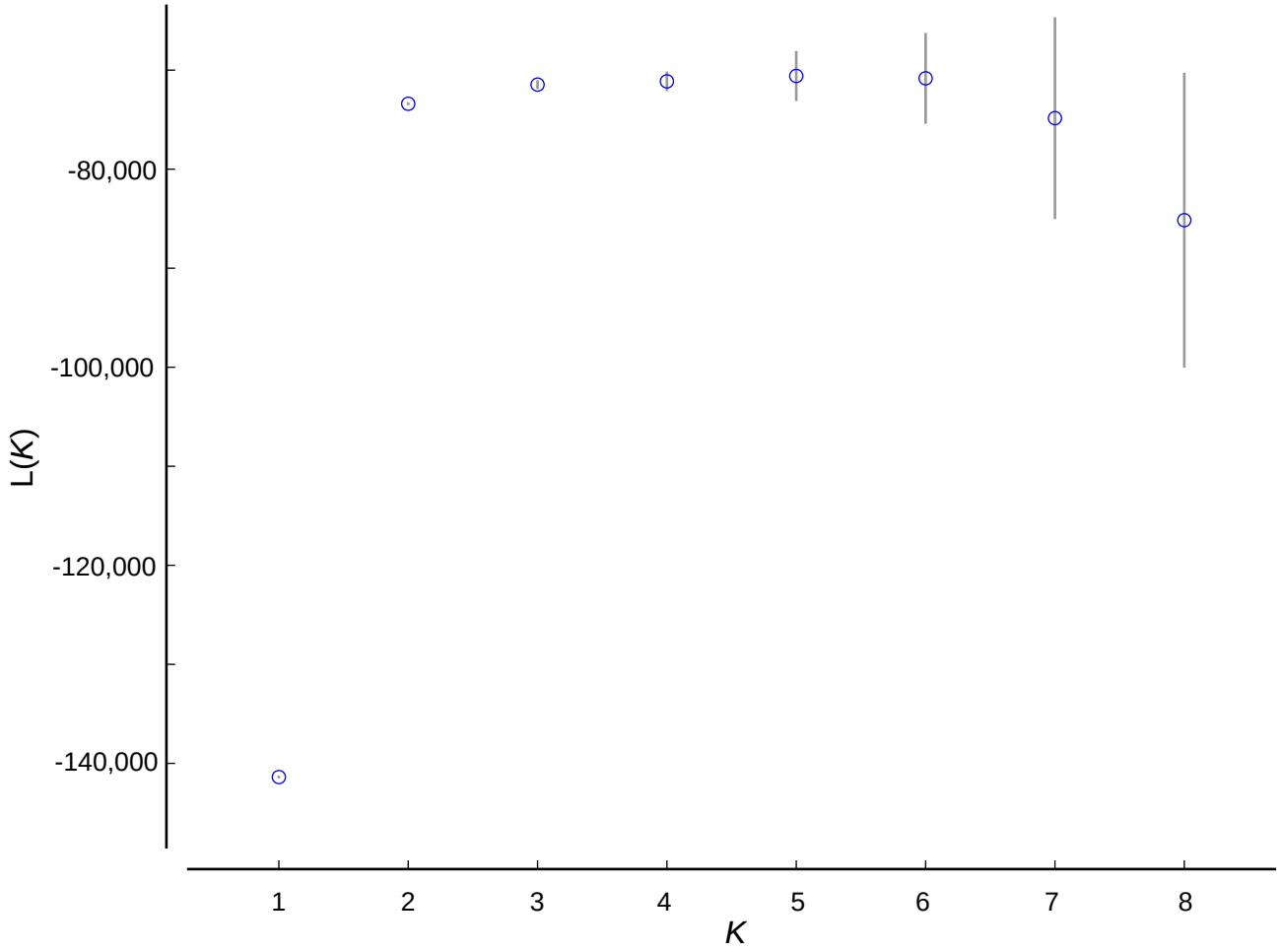


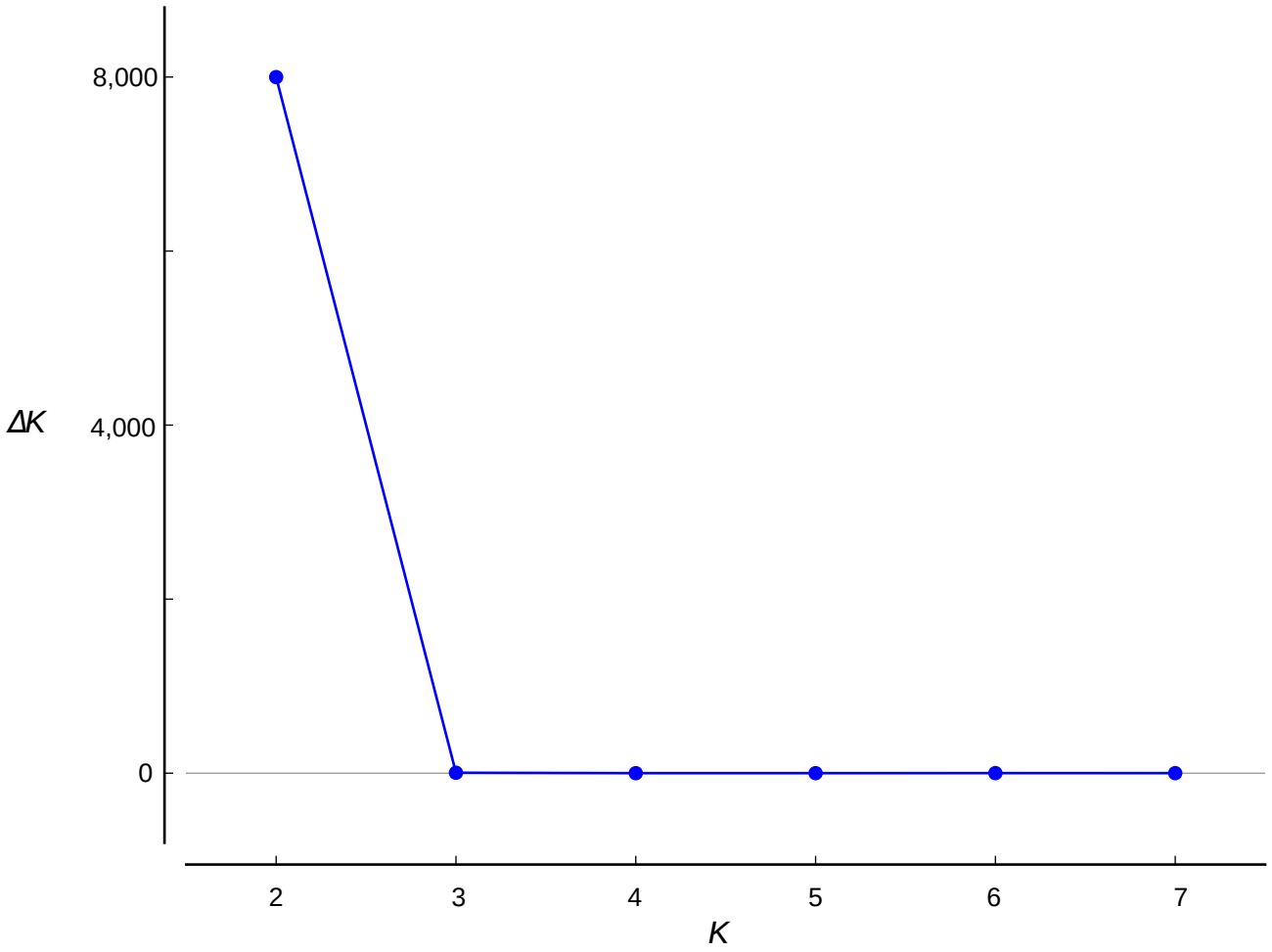


**File S4:** Statistics of the STRUCTURE analyses of the RAD data.

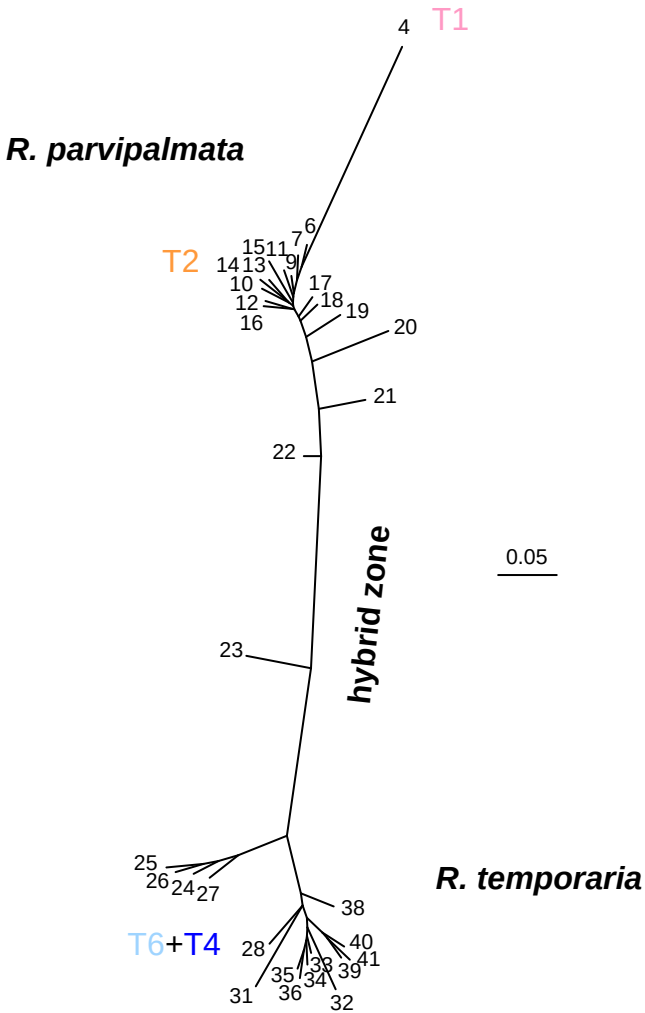


**File S5a:** Neighbor-Joining tree of pairwise genetic distances ($F_{st}$) among populations. The estimates are provided in File S5b.

**File S5b:** Pairwise genetic distances ($F_{st}$) between common frog populations from northern Spain. Color code reflects the three main nuclear groups (see Fig. 1). Populations 6–9 and 17–24 are admixed.

| | 4 | 6 | 7 | 9 | 10 | 11 | 12 | 13 | 14 | 15 | 16 | 17 | 18 | 19 | 20 | 21 | 22 | 23 | 24 | 25 | 26 | 27 | 28 | 31 | 32 | 33 | 34 | 35 | 36 | 38 | 39 | 40 | 41 |
|---|---|---|---|---|---|---|---|---|---|---|---|---|---|---|---|---|---|---|---|---|---|---|---|---|---|---|---|---|---|---|---|---|---|
| 4 | - | | | | | | | | | | | | | | | | | | | | | | | | | | | | | | | | |
| 6 | 0.23 | - | | | | | | | | | | | | | | | | | | | | | | | | | | | | | | | |
| 7 | 0.24 | 0.05 | - | | | | | | | | | | | | | | | | | | | | | | | | | | | | | | |
| 9 | 0.26 | 0.06 | 0.05 | - | | | | | | | | | | | | | | | | | | | | | | | | | | | | | |
| 10 | 0.28 | 0.08 | 0.06 | 0.04 | - | | | | | | | | | | | | | | | | | | | | | | | | | | | | |
| 11 | 0.27 | 0.06 | 0.05 | 0.04 | 0.06 | - | | | | | | | | | | | | | | | | | | | | | | | | | | | |
| 12 | 0.28 | 0.07 | 0.06 | 0.05 | 0.05 | 0.05 | - | | | | | | | | | | | | | | | | | | | | | | | | | | |
| 13 | 0.28 | 0.08 | 0.07 | 0.05 | 0.05 | 0.06 | 0.06 | - | | | | | | | | | | | | | | | | | | | | | | | | | |
| 14 | 0.27 | 0.08 | 0.07 | 0.05 | 0.06 | 0.06 | 0.06 | 0.05 | - | | | | | | | | | | | | | | | | | | | | | | | | |
| 15 | 0.28 | 0.09 | 0.07 | 0.06 | 0.06 | 0.06 | 0.06 | 0.07 | 0.08 | - | | | | | | | | | | | | | | | | | | | | | | | |
| 16 | 0.28 | 0.08 | 0.06 | 0.06 | 0.06 | 0.06 | 0.05 | 0.05 | 0.06 | 0.06 | - | | | | | | | | | | | | | | | | | | | | | | |
| 17 | 0.27 | 0.07 | 0.07 | 0.06 | 0.06 | 0.06 | 0.05 | 0.06 | 0.06 | 0.07 | 0.05 | - | | | | | | | | | | | | | | | | | | | | | |
| 18 | 0.26 | 0.08 | 0.07 | 0.06 | 0.07 | 0.06 | 0.05 | 0.06 | 0.06 | 0.07 | 0.06 | 0.04 | - | | | | | | | | | | | | | | | | | | | | |
| 19 | 0.28 | 0.10 | 0.09 | 0.08 | 0.08 | 0.09 | 0.09 | 0.08 | 0.08 | 0.10 | 0.08 | 0.07 | 0.07 | - | | | | | | | | | | | | | | | | | | | |
| 20 | 0.30 | 0.15 | 0.15 | 0.13 | 0.12 | 0.14 | 0.14 | 0.12 | 0.14 | 0.13 | 0.14 | 0.14 | 0.12 | 0.13 | - | | | | | | | | | | | | | | | | | | |
| 21 | 0.29 | 0.15 | 0.15 | 0.14 | 0.13 | 0.15 | 0.14 | 0.12 | 0.13 | 0.16 | 0.14 | 0.12 | 0.12 | 0.11 | 0.15 | - | | | | | | | | | | | | | | | | | |
| 22 | 0.26 | 0.13 | 0.13 | 0.11 | 0.11 | 0.12 | 0.12 | 0.10 | 0.12 | 0.12 | 0.12 | 0.10 | 0.09 | 0.10 | 0.12 | 0.07 | - | | | | | | | | | | | | | | | | |
| 23 | 0.32 | 0.24 | 0.25 | 0.24 | 0.24 | 0.25 | 0.25 | 0.23 | 0.24 | 0.26 | 0.25 | 0.22 | 0.19 | 0.21 | 0.23 | 0.16 | 0.10 | - | | | | | | | | | | | | | | | |
| 24 | 0.45 | 0.43 | 0.45 | 0.45 | 0.46 | 0.47 | 0.46 | 0.46 | 0.46 | 0.47 | 0.46 | 0.43 | 0.39 | 0.42 | 0.44 | 0.36 | 0.28 | 0.13 | - | | | | | | | | | | | | | | |
| 25 | 0.47 | 0.46 | 0.47 | 0.47 | 0.48 | 0.49 | 0.48 | 0.48 | 0.49 | 0.50 | 0.49 | 0.46 | 0.42 | 0.44 | 0.47 | 0.38 | 0.30 | 0.13 | 0.05 | - | | | | | | | | | | | | | |
| 26 | 0.47 | 0.45 | 0.47 | 0.47 | 0.48 | 0.49 | 0.48 | 0.48 | 0.48 | 0.50 | 0.48 | 0.45 | 0.42 | 0.44 | 0.46 | 0.38 | 0.30 | 0.14 | 0.07 | 0.05 | - | | | | | | | | | | | | |
| 27 | 0.42 | 0.42 | 0.44 | 0.44 | 0.45 | 0.48 | 0.45 | 0.47 | 0.49 | 0.49 | 0.48 | 0.44 | 0.40 | 0.43 | 0.46 | 0.37 | 0.28 | 0.13 | 0.08 | 0.07 | 0.08 | - | | | | | | | | | | | |
| 28 | 0.47 | 0.46 | 0.47 | 0.47 | 0.48 | 0.50 | 0.49 | 0.49 | 0.50 | 0.51 | 0.50 | 0.47 | 0.43 | 0.45 | 0.48 | 0.39 | 0.31 | 0.15 | 0.10 | 0.08 | 0.07 | 0.10 | - | | | | | | | | | | |
| 31 | 0.51 | 0.51 | 0.52 | 0.52 | 0.53 | 0.55 | 0.53 | 0.54 | 0.55 | 0.56 | 0.55 | 0.52 | 0.48 | 0.50 | 0.53 | 0.45 | 0.36 | 0.21 | 0.18 | 0.17 | 0.15 | 0.18 | 0.11 | - | | | | | | | | | |
| 32 | 0.49 | 0.49 | 0.51 | 0.51 | 0.52 | 0.54 | 0.52 | 0.53 | 0.54 | 0.55 | 0.54 | 0.51 | 0.46 | 0.49 | 0.51 | 0.44 | 0.35 | 0.20 | 0.16 | 0.15 | 0.13 | 0.17 | 0.10 | 0.14 | - | | | | | | | | |
| 33 | 0.46 | 0.46 | 0.47 | 0.47 | 0.48 | 0.50 | 0.48 | 0.49 | 0.50 | 0.51 | 0.50 | 0.47 | 0.43 | 0.45 | 0.48 | 0.40 | 0.31 | 0.16 | 0.12 | 0.11 | 0.09 | 0.12 | 0.06 | 0.11 | 0.08 | - | | | | | | | |
| 34 | 0.48 | 0.47 | 0.48 | 0.48 | 0.49 | 0.50 | 0.49 | 0.49 | 0.49 | 0.51 | 0.50 | 0.47 | 0.43 | 0.46 | 0.48 | 0.40 | 0.32 | 0.17 | 0.12 | 0.11 | 0.09 | 0.10 | 0.06 | 0.11 | 0.07 | 0.04 | - | | | | | | |
| 35 | 0.48 | 0.47 | 0.48 | 0.49 | 0.50 | 0.51 | 0.50 | 0.49 | 0.50 | 0.51 | 0.50 | 0.47 | 0.43 | 0.46 | 0.48 | 0.40 | 0.32 | 0.17 | 0.12 | 0.11 | 0.09 | 0.11 | 0.06 | 0.11 | 0.07 | 0.04 | 0.04 | - | | | | | |
| 36 | 0.49 | 0.48 | 0.49 | 0.50 | 0.51 | 0.51 | 0.51 | 0.50 | 0.51 | 0.52 | 0.51 | 0.48 | 0.44 | 0.47 | 0.49 | 0.41 | 0.33 | 0.18 | 0.13 | 0.12 | 0.10 | 0.12 | 0.07 | 0.11 | 0.07 | 0.05 | 0.05 | 0.04 | - | | | | |
| 38 | 0.42 | 0.42 | 0.44 | 0.44 | 0.45 | 0.48 | 0.45 | 0.47 | 0.49 | 0.49 | 0.48 | 0.45 | 0.41 | 0.43 | 0.46 | 0.38 | 0.29 | 0.16 | 0.13 | 0.12 | 0.11 | 0.17 | 0.09 | 0.13 | 0.10 | 0.08 | 0.06 | 0.06 | 0.06 | - | | | |
| 39 | 0.47 | 0.46 | 0.47 | 0.47 | 0.48 | 0.50 | 0.49 | 0.48 | 0.49 | 0.50 | 0.49 | 0.46 | 0.43 | 0.45 | 0.47 | 0.39 | 0.32 | 0.18 | 0.13 | 0.12 | 0.11 | 0.13 | 0.08 | 0.12 | 0.09 | 0.07 | 0.06 | 0.06 | 0.06 | 0.07 | - | | |
| 40 | 0.44 | 0.43 | 0.45 | 0.45 | 0.46 | 0.48 | 0.46 | 0.47 | 0.49 | 0.49 | 0.48 | 0.45 | 0.41 | 0.44 | 0.46 | 0.38 | 0.30 | 0.17 | 0.14 | 0.13 | 0.11 | 0.16 | 0.09 | 0.13 | 0.10 | 0.08 | 0.07 | 0.06 | 0.06 | 0.08 | 0.05 | - | |
| 41 | 0.46 | 0.45 | 0.47 | 0.47 | 0.48 | 0.49 | 0.48 | 0.48 | 0.48 | 0.50 | 0.49 | 0.46 | 0.42 | 0.44 | 0.46 | 0.39 | 0.31 | 0.18 | 0.14 | 0.13 | 0.11 | 0.14 | 0.08 | 0.13 | 0.09 | 0.07 | 0.06 | 0.06 | 0.06 | 0.07 | 0.04 | 0.05 | - |

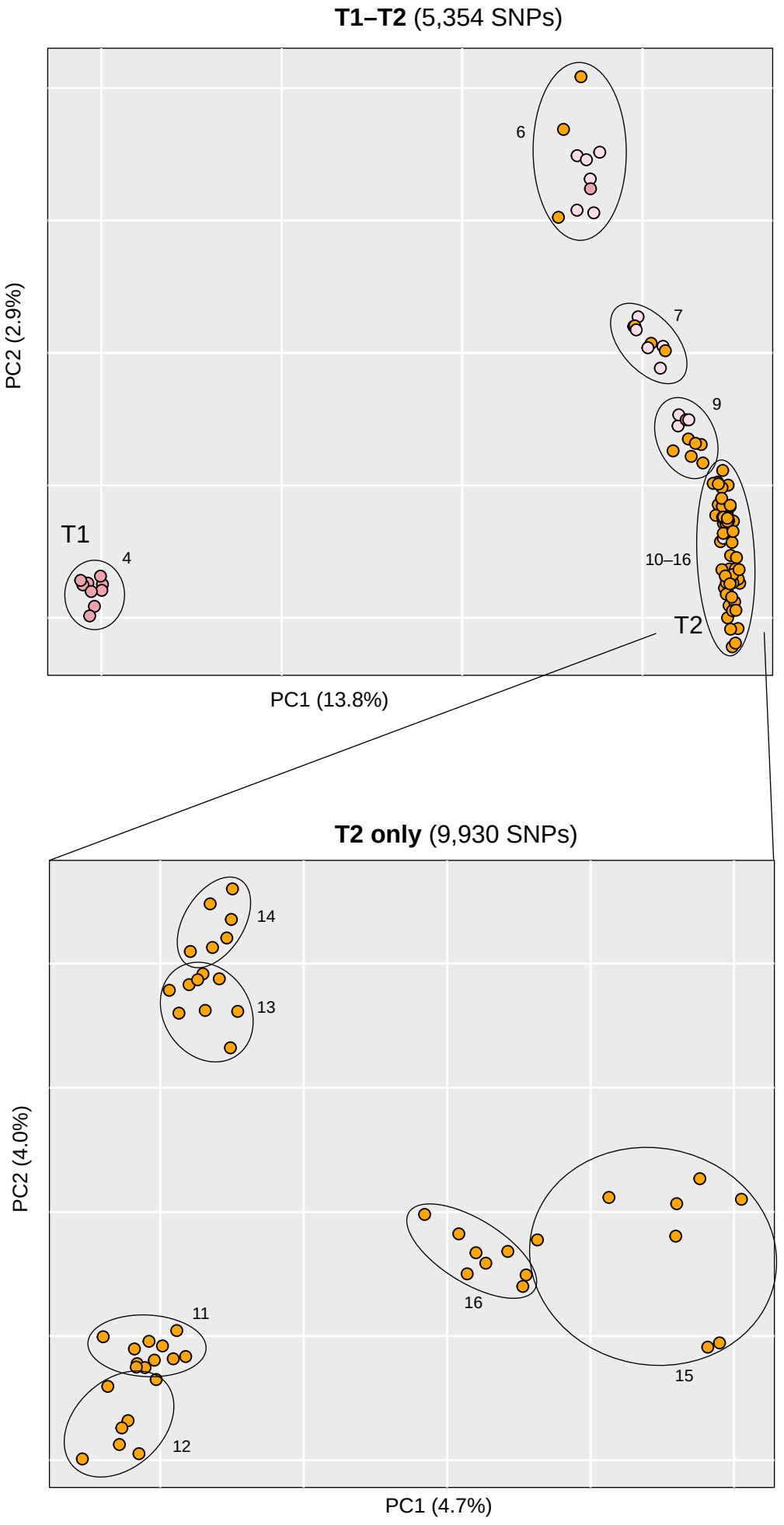


**File S6a:** Intraspecific PCA of *R. parvipalmata,* including all populations (top), and pure populatons from the Asturian lineage T2. Colors indicate the mitochondrial lineages (dark pink: T1a; light pink: T1b; orange: T2). Localities or groups of localities are encircled.

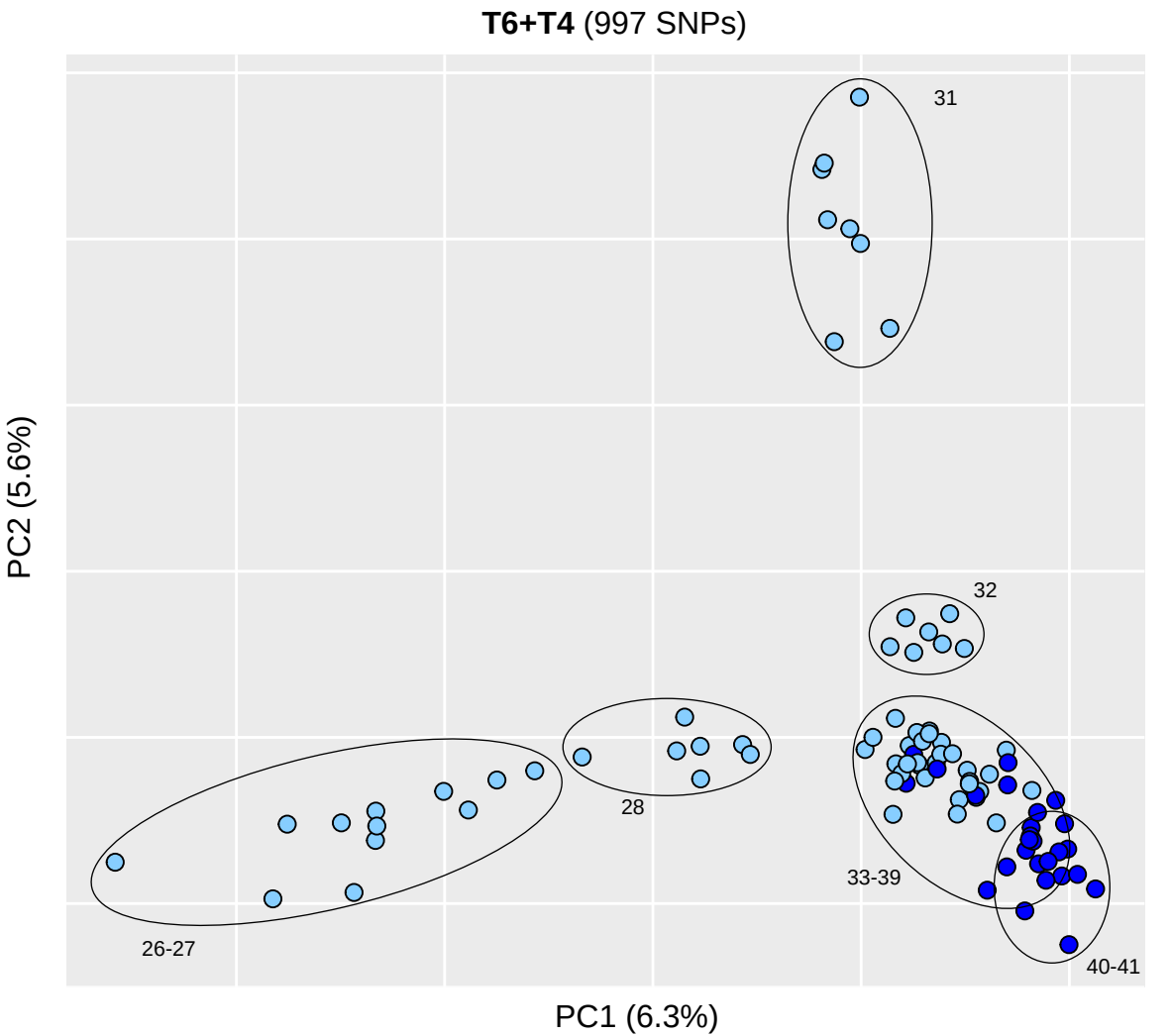


**File S6b:** Intraspecific PCA of *R. temporaria* populations from N-Spain. Colors indicate the mitochondrial lineages (blue: T4; light blue: T6). Localities or groups of localities are encircled.

**File S7:** Statistics on the bioclimatic models built for common frogs, combining all lineages (*R. temporaria* s. l.), separately for each species identified (*R. temporaria* and *R. parvipalmata*), and for the main mitochondrial lineages of *R. temporaria* in northern Spain (T4 and T6).

| | ***R. temporaria s. l.*** | ***R. temporaria*** | ***R. parvipalmata*** | **T4** | **T6** |
|---|---|---|---|---|---|
| Number of localities | 5,109 | 4,893 | 109 | 87 | 36 |
| AUC | 0.796±0.008 | 0.799±0.004 | 0.994±0.002 | 0.989±0.009 | 0.998±0.001 |
| Altitude | 0 | 0 | 0.4 | 1.3 | 0.3 |
| Aridity index | 71.4 | 67.7 | 5.2 | 17.7 | 13.1 |
| Annual mean temperature (Bio1) | 1.4 | 2.4 | 0.4 | 0.4 | 1.5 |
| Annual precipitation (Bio12) | 0 | 0.1 | 3.1 | 2.2 | 1.6 |
| Aspect | 0 | 0.1 | 1.1 | 0.4 | 0.1 |
| Exposition | 0 | 0 | 0.7 | 0.7 | 0.1 |
| Habitat heterogeneity | 1.1 | 1.3 | 2.7 | 3.6 | 2.0 |
| Mean diurnal range (Bio2) | 7.7 | 8.6 | 2.9 | 1.5 | 1.2 |
| Mean temperature of wettest quarter (Bio8) | 1.4 | 2.0 | 0.3 | 1.0 | 0.6 |
| Precipitation seasonality (Bio15) | 1.5 | 1.3 | 3.8 | 10.1 | 3.6 |
| Precipitation of warmest quarter (Bio18) | 0.1 | 0.1 | 13.6 | 1.4 | 0.2 |
| Slope | 0.4 | 0.4 | 20.3 | 15.3 | 35.4 |
| Temperature annual range (Bio7) | 11.8 | 12.6 | 41.3 | 40.3 | 35.9 |
| Terrain roughness index | 0.7 | 0.6 | 1.5 | 1.6 | 1.0 |
| Tree coverage percent | 2.3 | 2.8 | 2.7 | 2.4 | 3.4 |

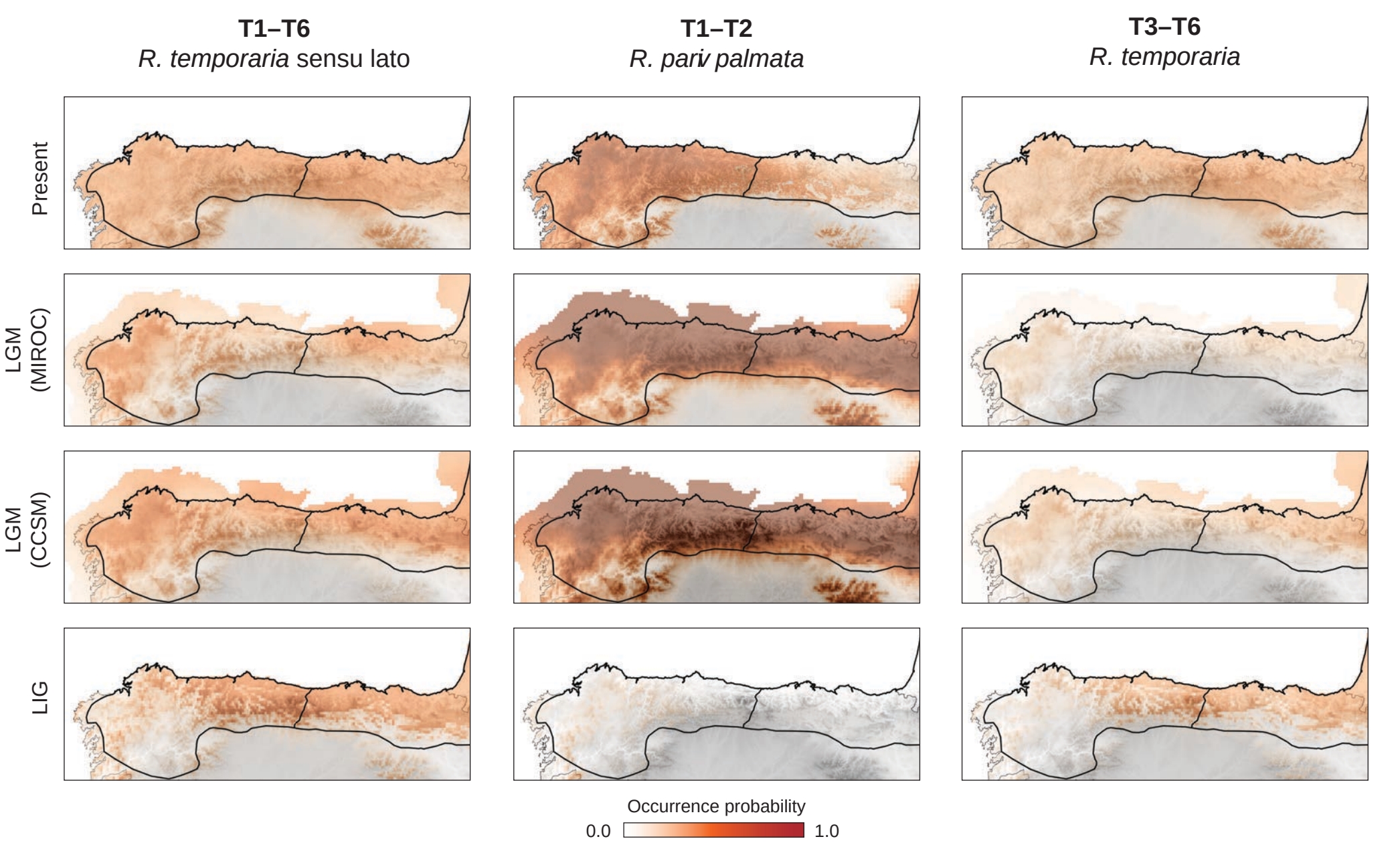


**File S8a:** Projections of past (LIG: last interglacial; LGM: last glacial maix mum) and present distributions obtained with models built from occurrence data across the entire ranges, seperately for *R. pariv palmata* and *R. temporaria*, and for both of them grouped (*R. temporaria* sensu lato). The corresponding mtDNA lineages are indicated. Model performance (AUC) is proiv ded for each.

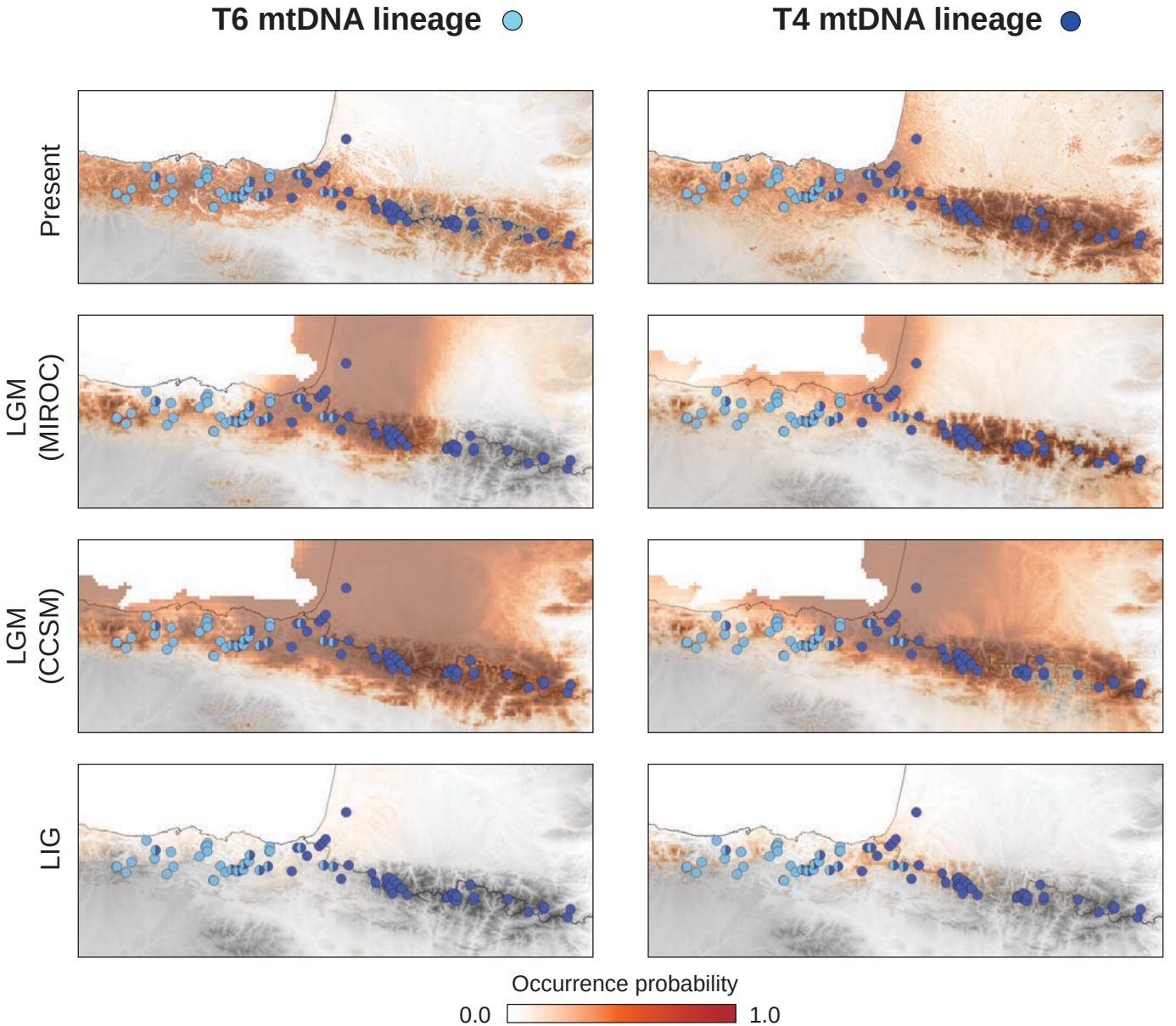


**File S8b:** Projections of past (LIG: last interglacial; LGM: last glacial maximum) and present distributions for the mitochondrial lineages T6 and T4. Model performance (AUC) is provided for each. Known lineage distributions are shown by the occurrence data used in the models (circles), combining our study with Vences et al. (2013, 2017).

**File S9:** P-values associated to the correlations between genetic indices (*D*: cyto-nuclear discordance; *AI*: admixture index; $H_o$: observed heterozygosity at RAD loci; π: nucleotide diversity at the mitochondrial *cyt-b*) of each population and their climate suitability (probability of occurrence) and instability (variance in the probabilities of occurrence between periods), as predicted from the SDMs. The number of sample sites for each comparison is provided (*N*). Analyses were performed separately for *R. temporaria* (T6+T4) and *R. parvipalmata* (T1–T2), their transition zone (T2+T6), and for all populations together (all range). The SDM used (taxon-specific or grouping both taxa, i. e. *R. temporaria* s. l.) is indicated. The significance threshold is provided for each set of tests, after bonferroni corrections. For *R. parvipalmata* (T1–T2), the MIROC predictions were identical (1.0) for all populations and could not be tested.

| | | ***D*** | ***AI*** | **$H_o$** | **π** |
|---|---|---|---|---|---|
| **T6+T4** | *N* | 13 | 13 | 13 | 14 |
| *R. temporaria* | climate instability | 0.10 | - | 0.45 | 0.90 |
| significant if *P*<0.0033 | present occurrence | 0.04 | - | 0.59 | 0.59 |
| | LGM occurrence (MIROC) | 0.17 | - | 0.20 | 0.34 |
| | LGM occurrence (CCSM) | 0.03 | - | 0.25 | 0.85 |
| | LIG occurrence | 0.15 | - | 0.44 | 0.94 |
| **T1-T2** | *N* | 11 | 11 | 11 | 12 |
| *R. parvipalmata* | climate instability | 0.15 | 0.07 | 0.39 | 0.34 |
| significant if *P*<0.0031 | present occurrence | 0.25 | 0.26 | 0.41 | 0.19 |
| | LGM occurrence (MIROC) | - | - | - | - |
| | LGM occurrence (CCSM) | 0.54 | 0.29 | 0.73 | 0.75 |
| | LIG occurrence | 0.71 | 0.54 | 0.03 | 0.70 |
| **T2+T6** | *N* | 20 | 20 | 20 | 21 |
| *R. temporaria* s. l. | climate instability | 0.12 | 0.20 | 0.32 | 0.74 |
| significant if *P*<0.0025 | present occurrence | 0.55 | 0.63 | 0.74 | 0.04 |
| | LGM occurrence (MIROC) | 0.61 | 0.75 | 0.65 | 0.99 |
| | LGM occurrence (CCSM) | 0.22 | 0.04 | 0.24 | 0.52 |
| | LIG occurrence | 0.45 | 0.71 | 0.40 | 0.67 |
| **All range** | *N* | 33 | 33 | 33 | 35 |
| *R. temporaria* s. l. | climate instability | 0.51 | 0.16 | 0.17 | 0.70 |
| significant if *P*<0.0025 | present occurrence | 0.13 | 0.79 | 0.42 | 0.99 |
| | LGM occurrence (MIROC) | 0.88 | 0.19 | 0.15 | 0.35 |
| | LGM occurrence (CCSM) | 0.58 | 0.01 | 0.01 | 0.90 |
| | LIG occurrence | 0.95 | 0.77 | 0.08 | 0.34 |

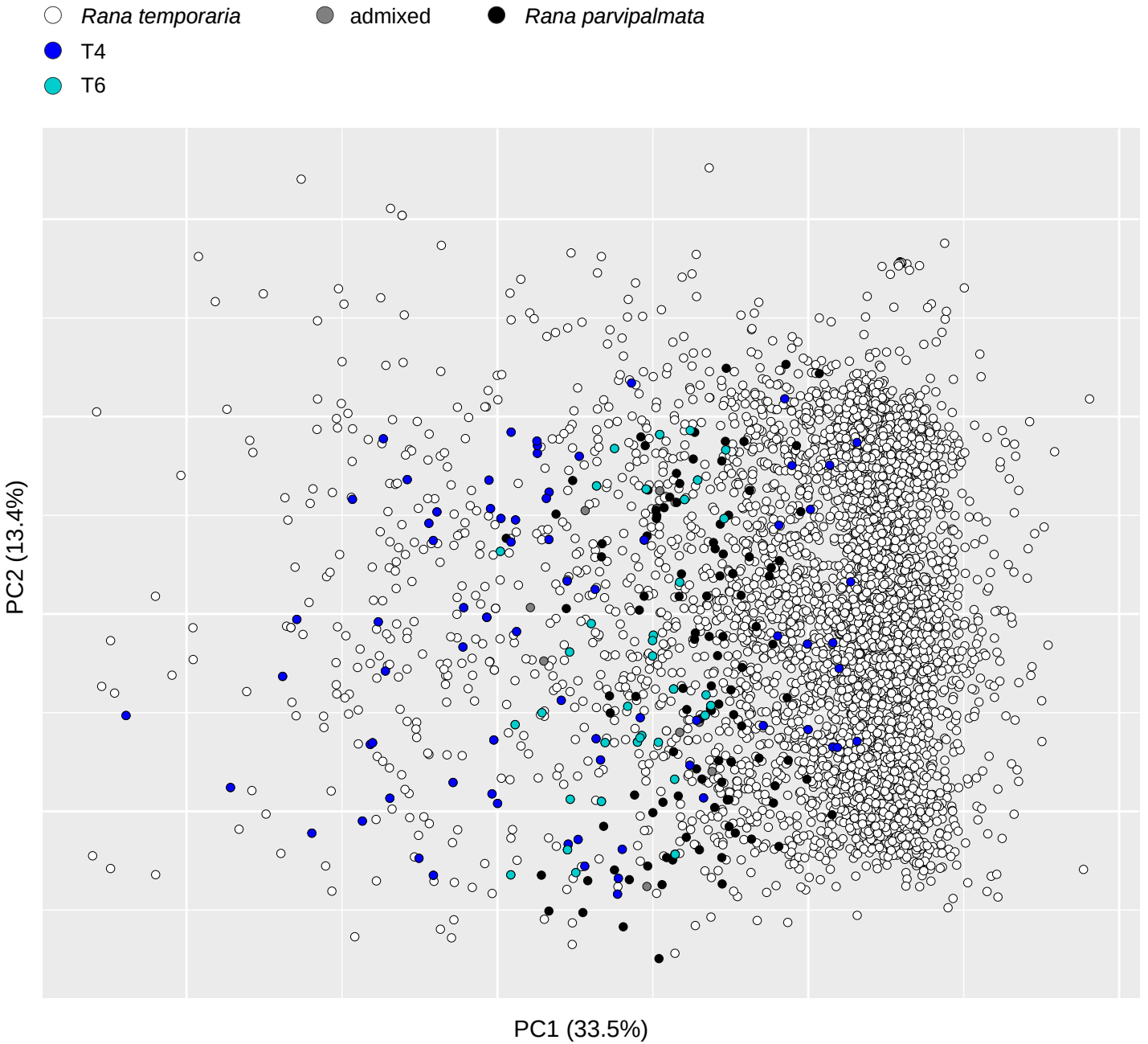


**File S10:** PCA on the variables retained in the climatic models at localities where common frogs are present.